


Review

Influencing Factors on Petrography Interpretations in Provenance Research—A Case-Study Review

Carita Augustsson 

Department of Energy Resources, University of Stavanger, 4021 Stavanger, Norway; carita.augustsson@uis.no

Abstract: The use of framework petrography is a common initial step in provenance research of sand and sandstone. The data tend to be interpreted based on the three main components quartz, feldspar, and lithic fragments. Surprisingly often, this is done without taking other influencing factors than the tectonic setting of the catchment and/or the surroundings of the depositional basin into account. Based on a database of 14 studies with approximately 900 petrographic data points from sand and sandstone, this study demonstrates quantitative effects on the apparent composition resulting from both geological and non-geological biases. The study illustrates sandstone-classification differences based on different specifications of the three end-members quartz, feldspar, and lithic or rock fragments, how the point-counting method can affect the apparent petrographic composition of sandstone, how sorting and facies bias may be differentiated from a climate or provenance signal, and how bias due to diagenetic effects can be minimised. In conclusion, both geological and non-geological biases should be considered for provenance studies that include petrographic data.

Keywords: siliciclastic sedimentary petrography; provenance; sorting; facies; diagenesis; point counting



Citation: Augustsson, C. Influencing Factors on Petrography Interpretations in Provenance Research—A Case-Study Review. *Geosciences* **2021**, *11*, 205. <https://doi.org/10.3390/geosciences11050205>

Academic Editors: Emilia Le Pera, Consuele Morrone and Jesus Martinez-Frias

Received: 29 March 2021
Accepted: 6 May 2021
Published: 8 May 2021

Publisher's Note: MDPI stays neutral with regard to jurisdictional claims in published maps and institutional affiliations.



Copyright: © 2021 by the author. Licensee MDPI, Basel, Switzerland. This article is an open access article distributed under the terms and conditions of the Creative Commons Attribution (CC BY) license (<https://creativecommons.org/licenses/by/4.0/>).

1. Introduction

The use of framework petrography is a common initial step in provenance research of sand and sandstone. Interpretations often lean on the tectonically-based provenance-discriminative schemes of Dickinson and Suczek [1] or on modified versions of them (Figure 1) [2,3]. This can lead to interpretations towards, e.g., tectonic environments and developments in the catchment area at the time of deposition and of that of the basin if it is part of the same tectonic regime as the catchment (e.g., [1,4,5]). Climate, the other major basin-external factor for sedimentation and sediment composition, too often either is not accounted for or even interpreted separately with the same petrographic data that are used for tectonic considerations, though many studies take both factors properly into account (e.g., [5–9]).

In addition to the external factors, processes that operate during the complete sedimentary cycle have the capability to modify the petrographic composition of sedimentary material (e.g., [10,11]). This includes pre-depositional weathering of source rocks and detrital material during temporal storage in the transport system [7,12], physical sorting during transport and deposition, diagenesis, as well as weathering after uplift. Additionally, sampling of weathered material or selective sampling (e.g., [11,13,14]) can lead to the analysis of material that is less representative for the source than preferred. Such non-geological (artificial) compositional (and analytical) biases have been particularly focused on for single-grain analysis in provenance research (e.g., [15–17]). Apparent differences in sediment compositions can also appear for the same samples based on the use of different point-counting methods or due to subjective interpretation of components for different operators (e.g., [18–20]).

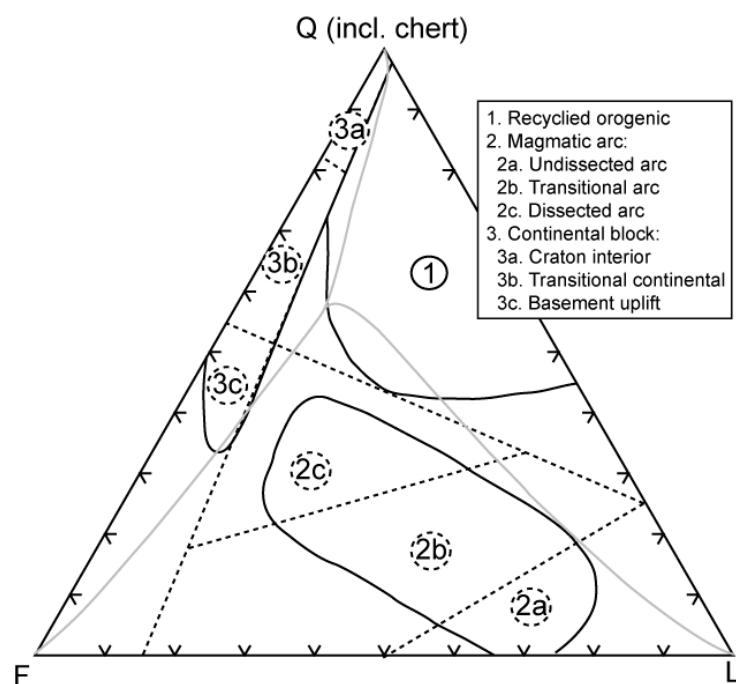


Figure 1. One of the most commonly used petrographic provenance-discriminative schemes, including the original diagram of Dickinson and Suczek [1] (solid black lines), and the modified versions of Dickinson et al. [2] (dashed black lines) and Weltje [3] (grey lines). For the use of the discrimination fields, the Gazzi–Dickinson point-counting method should be used with a grain-matrix limit of 63 μm . Only aphanitic lithic fragments are included in the lithic-fragment pool; carbonate clasts are excluded. Q: quartz (both monocrystalline and polycrystalline grains); F: feldspar; L: lithic fragments (excluding carbonate and other mono-mineralic polycrystalline grains). “Chert” encompasses both sedimentary and volcanic microcrystalline quartz.

Many publications deal with the quantitative effect of basin-external factors on sedimentary framework petrography (e.g., [1,4,21–23]). Basin-internal factors also are treated, though possibly less frequently (e.g., [24–29]). Methodological effects are also not focused on in the literature, although some point-counting-method comparisons have been performed (e.g., [18,30,31]).

This review aims to give an overview of apparent compositional differences of sandstone that may emerge due to basin-internal and non-geological factors, with examples from literature data. The review touches upon sorting and facies, diagenesis, as well as operator bias, and the use of different point-counting methods for classification and provenance interpretation.

2. Materials and Methods

The data set was composed of approximately 900 mostly sand and sandstone samples (the full data set is available as Supplementary data, Table S1). Less than 40 samples (minor proportions in Götze [32], Mørk [33], von Eynatten and Gaupp [34], De Ros et al. [35], Lippmann [36], Olivarius et al. [37]) that are formally silt or conglomerates were included; they are mentioned in the text only when it is relevant for the discussion. The data include a sequence from the Permian to Palaeogene of Northern Europe (from Germany in the south to the Barents Sea in the north) with a transition from Permo–Triassic tectonically passive to rift-dominated continental and Jurassic to Cretaceous marine rift basins, to Palaeogene passive-margin marine environments [20,32,33,36–40]. They also include coastal Cambrian passive-margin sandstone from Scandinavian Baltica [41–43], Silurian–Devonian intracratonic basin sandstone from the Paraná Basin in Brazil [35], Cretaceous Alpine deposits [34,44], rift-related Iberian Cretaceous to Pyrenean Palaeogene continental to marine

deposits [45,46], and recent intracontinental sand from central Spain [47]. The material represents fluvial, aeolian, lacustrine, deltaic, coastal, shallow-marine, slope, and deep-marine depositional environments. Thirty-seven percent of the samples are from outcrops, and the remaining are from wells at sampling depths of 24–5200 m. When specified in the original publications, the maximum burial depths were estimated to 1200–2200 m (Table S1). In Table S1, grain size and textural information are provided, according to Wentworth [48], Powers [49], Folk and Ward [50], Krumbein and Sloss [51], and Longiaru [52]. When specified, the studies were done with either the Gazzi–Dickinson point-counting method [53] (or a modification of it) or the Indiana method [54]. In addition, different grain-size limits for grain vs. matrix were used.

The Gazzi–Dickinson method assumes that crystals of sand size within rock fragments are identified as the mineral type in the crosshair during the counting (part of phaneritic lithic or rock fragments of Dickinson [53]). Cherty grains (microcrystalline quartz) are counted as quartz, and carbonate clasts are not considered [53]. Any impurities of other minerals in feldspar or quartz grains (including chert) lead to these being classified as lithic fragments [18] (aphanitic lithic or rock fragments of Dickinson [53]). The limit between matrix and grains is set at 63 μm . The Indiana method (also known as the “traditional method”) assumes that a grain type is defined based on its main components of >90%, such that, for instance, a quartz grain can contain up to 10% of other mineral types [54]. Alternatively, at least two phases in the grain should be >63 μm . Polycrystalline quartz, including cherty grains and carbonate clasts, are included in the rock-fragment pool [54,55]. Similar to the Gazzi–Dickinson method, the grain-matrix cut-off is set at 63 μm , and only sand grains are counted. The term lithic fragment is used in this contribution when referring to aphanitic clasts in accordance with the Gazzi–Dickinson method and rock fragments when referring undifferentiated to aphanitic and phaneritic clasts in accordance with the Indiana method.

In the data set, Arribas et al. [47] and Caja et al. [46] used the Gazzi–Dickinson method with separate classes for carbonate clasts and sand-sized quartz, feldspar, and mica crystals in rock fragments. Lorentzen et al. [42,43] and Ärlebrand [40] used the Gazzi–Dickinson method but applied a 30 μm and 20 μm matrix cut-off, respectively. von Eynatten and Gaupp [34] and Augustsson et al. [20] used a modified Gazzi–Dickinson method with all rock fragments counted as such. Caja Rodríguez [45] is the only study specifying the use of the Indiana method. The other studies do not mention the counting method or the matrix-size limit. Feldspar that in the original publications was reported as being dissolved or altered were included in provenance-appropriate feldspar categories, irrespective of applied point-counting method.

The Gazzi–Dickinson-counted data of Arribas et al. [47] and Caja et al. [46] were recalculated to results equivalent to the Indiana method (without being able to apply the 90% and the alternative two-sand-sized-components rules for the mineralogical composition of rock fragments). The data also were recalculated from the sandstone classification scheme of Garzanti [23] to (almost) the McBride’s [56] classification scheme (without being able to apply his 20 μm matrix cut-off).

3. Non-Geological Biases

3.1. Operator Bias

Both the choice of point-counting method and the definition of the used compositional end members strongly can affect the apparent compositional result. Many sediment-petrographic studies on provenance only focus on the mineralogical framework, reporting to a limited degree on diagenetic phases, mineral alterations, and dissolutions that would be helpful for the reconstruction of the sediment composition at the time of deposition. Others focus more on diagenetic processes than on provenance, thus presenting detailed information on the intergranular volume and mineralogical alterations and dissolutions, giving only fragmentary information on the framework composition (cf. the range of petrographic details, e.g., in Lorentzen et al. [42,43]). A different focus alone may lead to

the use of different compositional and textural categories for the petrographic results and thus different classification of the same components. For instance, does feldspar include only detrital, unaltered feldspar, or also ceritised and partly dissolved feldspar grains? Should albitised feldspar be included in the plagioclase pool, or should those grains be investigated for their original potassium-rich or calcium-rich feldspar variant? Such decisions may influence the provenance interpretations. The identification of mineral phases is also subjective, causing challenges when comparing results from different operators (cf. [20,57,58]). To avoid such operator bias, Ingersoll et al. [18] let several operators point-count the same thin sections. Alternatively, careful standardisation between operators may need to be undertaken for a non-biased comparison of data from different operators.

3.2. Point-Counting-Method Bias

The common lack of specification of point-counting method in provenance studies highlights the challenge of comparing petrographic data that potentially have been counted with different methods. This is because of the differences in matrix-size cut-off and the way polycrystalline grains are classified and recalculated for provenance or classification diagrams. The Gazzi–Dickinson method classifies polycrystalline grains based on textural parameters. Phrased differently than in the method chapters, only aphanitic lithic fragments (L in the quartz-feldspar-lithic-fragment, QFL, diagram) are polycrystalline grains with components $<63\ \mu\text{m}$ in the crosshair, and phaneritic fragments are those including components $>63\ \mu\text{m}$ in the crosshair, with quartz and feldspar counted separately as long as they are of sand size (added to the Q and F categories of the QFL diagram) [53]. This distinction is not included in the Indiana point-counting method, which treats both fragment categories as one group of rock fragments, although the method assumes that the quartz or feldspar contents in the clasts are $<90\%$ [54] (originally included in the rock-fragment category of quartz-feldspar-rock-fragment diagrams, in this contribution they are shown in the same QFL diagrams as for the Gazzi–Dickinson method for simplicity). Therefore, results based on the Indiana method commonly cause a larger apparent compositional variation for different sand-grain sizes and a higher framework content of lithic/rock fragments than for data produced with the Gazzi–Dickinson method [18]. Hence, the use of compositional diagrams for illustration of petrographic results may indicate apparent, false compositional variations among data sets. Similarly, the use of discriminatory fields that were constructed for specific counting methods also can lead to inappropriate interpretations. In this contribution, it is illustrated how carbonate clasts, polycrystalline quartz, and sand-sized components in rock fragments all can affect the apparent composition of sand and sandstone.

3.3. Sandstone-Classification Effects on Method Bias

Several framework-component-based sandstone classification schemes have been suggested during the last century (see [59]). Those that are most used today all lean on the three compositional end members quartz, feldspar, and lithic or rock fragments (e.g., [23,56,60,61]). The older classification schemes focus on capturing the compositional variation of sandstone that occurs due to them being of different origin in terms of tectonic setting. Thus, for instance, arkose (or similar) includes a much larger compositional range than quartzarenite (or similar; see Figure 2 for the scheme of McBride [56]). Differently, Garzanti [23] aimed for a classification scheme that is neutral in respect to the origin. Therefore, in his scheme, the compositional ranges of quartzose and feldspathic sandstone are the same (Figure 2).

At first sight, it may seem straightforward to use any classification scheme for petrographic data of sandstone. However, each scheme involves restrictions in terms of grain size and component differences for the three end-member categories. To illustrate the effect, the classification schemes of McBride [56] and Garzanti [23] are compared here as they are different in several key aspects.

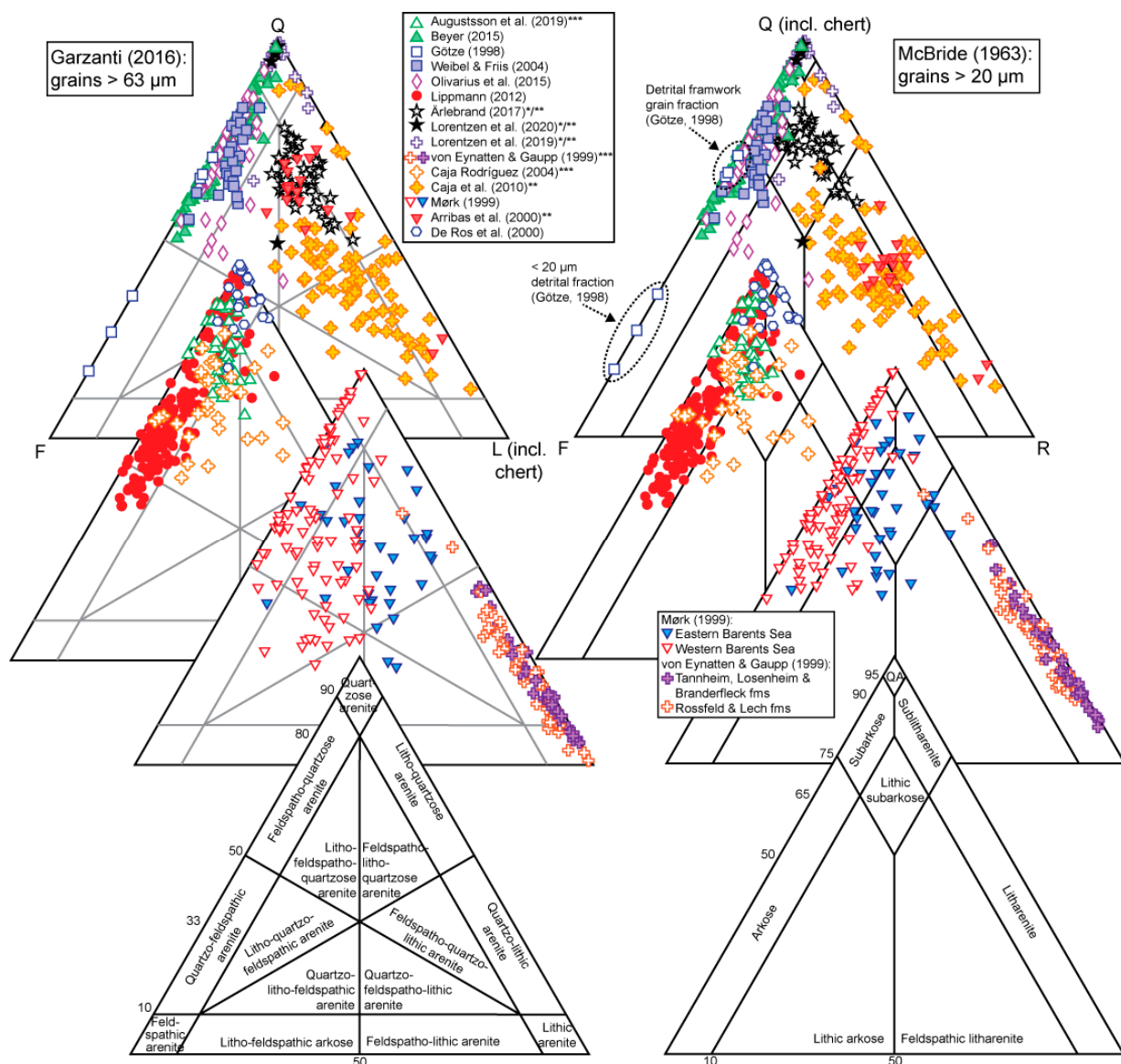


Figure 2. Sandstone classification of the rocks in the used data set based on the scheme of Garzanti [23] (left) and McBride [56] (right). All data are plotted, also the few samples that formally would be other rock types than sandstone. The grain-matrix cut-off for the sandstone of Götze [32] (for which the composition for the <20 µm fraction also is provided) is unknown. * Point-counting with a matrix limit of 20 or 30 µm; ** Gazzi–Dickinson point counting; *** Modified Gazzi–Dickinson (all rock fragments assigned to L) or Indiana point counting. The used counting methods for the other studies are unspecified. F: feldspar; L: lithic fragments (as defined by the Gazzi–Dickinson method, and including carbonate grains); Q: quartz (both monocrystalline and polycrystalline grains); QA: quartzarenite; R: rock fragments (including carbonate grains).

The sandstone classification scheme of McBride [56] includes eight different compositional fields and assumes that all particles larger than 20 µm are counted as grains; all other particles are considered to be part of the matrix. The 20 µm limit evolves from the possibility to identify the mineralogical composition of grains down to that size with a standard polarising microscope [56]. Thus, not only sand grains but also medium and coarse silt, as well as gravel, are considered. In addition, the classification scheme assumes that all quartz, including polycrystalline quartz (with cherty grains), are counted as quartz because a macroscopic differentiation between monocrystalline and polycrystalline quartz is challenging [56]. Similarly, all grains that are composed only of feldspar are included in the feldspar pool. The rock fragments in McBride’s [56] scheme include all particles with

more than one mineral phase as well as carbonate clasts. Other mono-mineralic grains are excluded.

The sandstone classification scheme of Garzanti [23] includes 15 different compositional fields (with five possible additional subfields for quartzose and feldspatho-quartzose sandstone [12,59]). Garzanti's [23] sandstone terminology captures compositional differences for feldspar-rich and lithic-fragment-rich sandstone better than quartz-rich sandstone (unless the supplementary terminology of Garzanti [59] is used), for which McBride's [56] terminology is more detailed (Figure 2). The scheme of Garzanti [23] builds on the Gazzi–Dickinson point-counting technique, although Garzanti [59] argues that a classification scheme should only be based on composition, not on texture or rock origin. However, therefore, the rock names are purely descriptive. Some other practical effects are that cherty grains are lithic fragments, other polycrystalline quartz grains are part of the quartz pool, and sand-sized crystals in rock fragments are to be counted as the mineral phase, not as lithic fragments. Similar to the Gazzi–Dickinson method, Garzanti [23] also only considered components >63 µm as grains. However, carbonate clasts are included in the lithic-fragment category, and the three end-members, quartz, feldspar, and lithic fragments, should account for at least 10% of the total sandstone framework.

Formally, only data produced with the appropriate method and using the given matrix limit should be used in the respective schemes. Despite this, all data are here plotted in both classification schemes to illustrate their general framework composition, as well as the differences between the two schemes. The data set in this study covers approximately half of the possible compositional spreads in the schemes (Figure 2). This represents much of the natural variation of sand and sandstone composition in nature [1,4,59].

Depending on chosen classification scheme, a group of samples may seem, based on name, either to all have a similar apparent composition or to illustrate a broad apparent compositional range. For instance, the sandstone from Weibel and Friis [38] is almost exclusively feldspatho-quartzose arenite or can partly be described as subarkose and partly as arkose (Figure 2). Differently, the sandstone of von Eynatten and Gaupp [34] is almost exclusively litharenite, or lithic arenite and quartzo-lithic arenite, thus, indicating an apparent larger variation when using the scheme of Garzanti [23].

Some data appear at different positions in the two diagrams because of the differences in the definition of end-member categories. This is particularly due to two factors:

- (1) Chert-rich sandstone will seem quartz-richer in McBride's [56] than in Garzanti's [23] scheme. In the data set, this is particularly visible for the continental to shallow-marine Triassic sandstone from the Barents Sea of Mørk [33] and the Cretaceous carbonate-rich gravity-flow sandstone from the Alps of von Eynatten and Gaupp [34], both of which include on average 8–9% cherty clasts (in the samples with such grains) in the detrital grain fractions. Whereas the Barents-Sea material mainly is subarkose and arkose (and partly lithic subarkose and lithic arkose) in the classification scheme of McBride [56], the compositional spread seems larger in Garzanti's [23] scheme, including mainly feldspatho-quartzose and litho-feldspatho-quartzose arenite (and some feldspatho-litho-quartzose and litho-quartzo-feldspathic arenite; Figure 2).
- (2) Sand-sized crystals in clasts that are counted as the mineral phase for the classification scheme of Garzanti [23] will lead to an apparent larger content of rock fragments when McBride's [56] scheme is used. This is illustrated by recalculation from Garzanti's [23] to (almost) McBride's [56] scheme (Figure 2) for the data of Arribas et al. [47] and Caja et al. [46]. The effect is the largest for the data of Arribas et al. [47], with mainly feldspatho-litho-quartzose arenite in the scheme of Garzanti [23] and litharenite to feldspathic litharenite in McBride's [56] scheme. This is because the studied sand contains, on average, 20% sand-sized quartz, feldspar, and mica crystals in rock fragments.

As McBride [56] applied a smaller matrix cut-off (20 µm) than Garzanti [23] (63 µm), the scheme of McBride [56] possibly is most appropriate for the studies reviewed here that used grain-matrix-size limits of 20 µm or 30 µm [40,42,43]. This is because different

grain sizes will produce sediment of different mineralogical compositions. As an extreme example, the data of Götze [32] from continental Triassic sandstone of Germany only include three samples, but these were investigated petrographically separately for the complete grain-size interval and for the <20 µm grain population for comparative reasons. The sandstone can be defined as feldspatho-quartzose arenite or arkose with higher quartz than feldspar content. The <20 µm fractions invariably has significantly higher feldspar than quartz contents (Figure 2), probably because feldspar easily breaks along its two cleavage planes to form silt. For quartz, the hardness and lack of cleavage cause less physical abrasion below the size of very fine sand, although also silty quartz grains form physically (e.g., [62,63]). The silt fraction of Götze [32] illustrates that the handling of silt-sized particles as detrital framework grains in sandstone might lead to an apparent feldspar-rich rock composition than if only sand grains are considered. Then, comparison of different data sets may be challenging.

3.4. Provenance Effect on Operator and Method Biases

The common use of one or several of the tectonically-based provenance-discrimination schemes of Dickinson and Suczek [1] may both help and hinder plausible interpretation, even if later reported weaknesses of the schemes are considered (e.g., [64,65]). As these schemes are designed for the Gazzi–Dickinson point-counting method, the use of the discriminatory fields may lead to inappropriate interpretations if a different counting method is used. This is also the case for the provenance-discriminative fields of Garzanti [59], who used the Gazzi–Dickinson-based sandstone-classification diagram of Garzanti [23] with carbonate clasts included in the lithic-fragment pool. Similarly, only data produced with the Indiana method should be used for the provenance-discriminative scheme for sand from igneous arcs of Kumon and Kiminami [66]. However, the general use of similar diagrams without discrimination fields will be applicable for data achieved from any point-counting method, as long as all data are produced from the same method, operator bias is avoided, and interpretations are based on comparative (i.e., relative, rather than absolute) sandstone compositions.

Rock fragments are an invaluable source of provenance information as they directly represent drainage lithologies. Their composition and texture frequently reveal detailed information about the source rocks (e.g., [19,59,67]). For this reason, second-order and third-order diagrams can be used to further increase the resolution to which clastic provenance can be reconstructed. For instance, Le Pera et al. [68] used a second-order diagram that includes plutonic, metamorphic, and sedimentary rock fragments (their ternary Rg-Rm-Rs diagram) to differentiate between sand of granitic and gneissic origin because both tend to produce quartz-feldspar-rich sand. For the lithic-fragment (or the complete rock-fragment) fraction, one of the probably most commonly used second-order schemes includes metamorphic (Lm), sedimentary (Ls), and volcanic grains (Lv) (e.g., [47,59,69]). More advanced grain schemes based on mineralogical and textural parameters for metamorphic [19] and volcanic [67,70–72] lithic or rock fragments allow for third-order discriminations. For instance, the proportions between basaltic lathwork (Lvl), andesitic microlithic (Lvmi), and vitric (Lv) textures can shed light on volcanic evolution and contribution from different volcanic centres [73], and the proportions between low-grade and high-grade metamorphic clasts may reveal arc unroofing [74]. For quantitatively reliable results from such sub-groups, a sufficient number of identified rock/lithic fragments of the compared categories need to be secured, for instance, with a separate point count that only focuses on rock or lithic fragments, such as was done by Ingersoll and Suczek [69] and Dorsey [74] for 150 and 300–400 lithic grains per sandstone sample, respectively. In this review, a second-order diagram that includes all igneous clasts (both plutonic and volcanic ones), sedimentary and metamorphic grains illustrates possible provenance misclassification of clay-mineral-rich clasts. Though, none of the studies used in this review included separate rock-fragment/lithic-fragment counts.

3.5. Cases Studies on Non-Geological Bias

3.5.1. Case 1—Operator Bias

Both Beyer [39] and Augustsson et al. [20] provided point-counts for early Triassic sandstone from Well Rockensußra 2/83 in Germany. The counting method was not described by Beyer [39], and Augustsson et al. [20] used a modified Gazzi–Dickinson method with all rock fragments assigned to the lithic-fragment pool. In addition, neither of the studies defined the grain-size cut-off for the matrix. Compared to Beyer [39], Augustsson et al. [20] claim higher ratios for monocristalline quartz in the total detrital quartz population and lower feldspar contents for similar facies and grain sizes at the same stratigraphic level (Solting Formation in Figure 3). Two samples were counted by two different operators, with an up to almost 10% difference in feldspar content in the framework and amounts of quartz types (Figure 3). In addition, in one of the samples, one operator did not find any rock fragments, whereas the other observed ca. 5% (Figure 3).

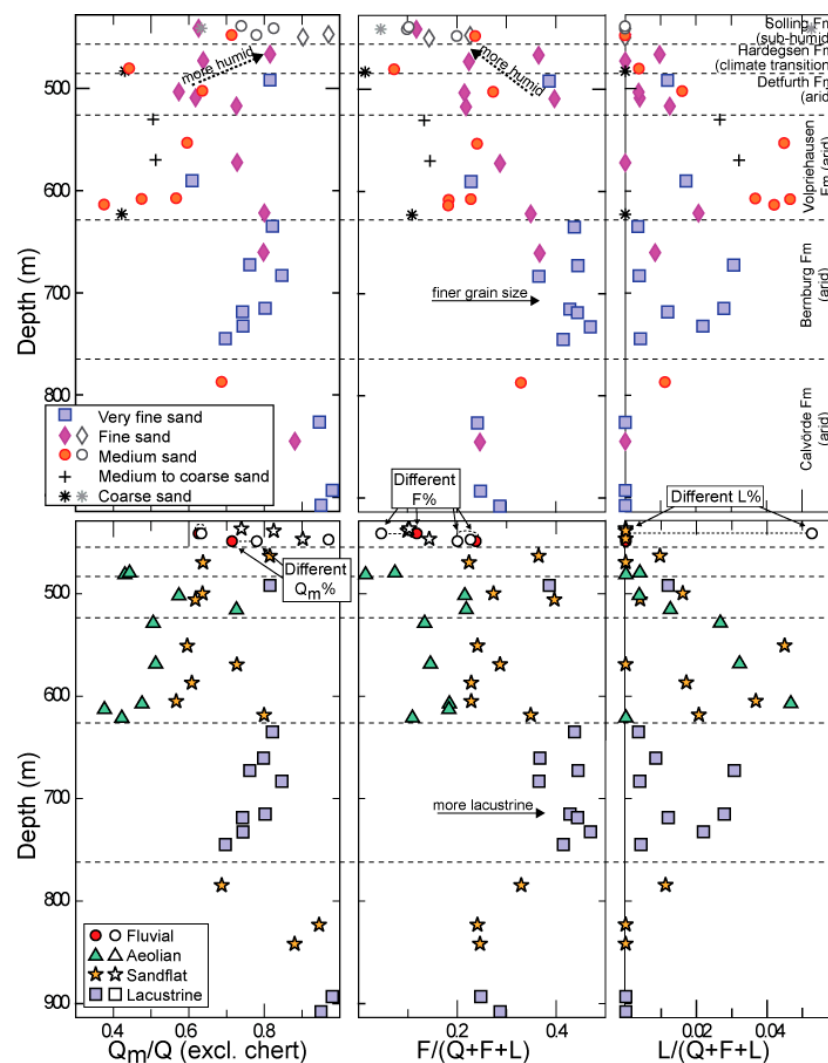


Figure 3. Compositional trends for Early Triassic sandstone in well Rockensußra 2/83 (Germany) based on data from Beyer [39] (coloured symbols) and Augustsson et al. [20] (white and grey symbols). Trends vs. both grain size and facies are shown. Identical samples are connected with dotted lines. Note that one sample was estimated as fine sandstone (200 μm) by Beyer [39], but coarse sandstone by Augustsson et al. [20]. F: feldspar; L: lithic/rock fragments (poly-mineralic grains only; no carbonate clasts were detected); Q: quartz (both monocristalline and polycristalline grains); Q_m : monocristalline Q.

The different point-counting results of Beyer [39] and Augustsson et al. [20] were most likely due to misinterpretation of some components by one or both operators. This is most obvious by the different classifications of lithic fragments, but also the difference in quartz types and feldspar contents may be affected. Bias due to the use of different point-counting methods also may be an explanation as they are described incompletely in the publications.

3.5.2. Cases 2a and 2b—Apparent Compositional Bias: Carbonate and Rock Fragments

The turbiditic Palaeogene foreland-basin sandstone from the Spanish Pyrenees [46] contains on average 35% carbonate clasts in the framework (equivalent to 80% of the rock fragments; leading to classification as hybrid arenite or calcilithite for the youngest units in the classification scheme of Zuffa [75]). The quartz fraction (including polycrystalline quartz, chert, and quartz in rock fragments) includes 30% polycrystalline grains. The amount of sand-sized quartz, feldspar, and mica crystals in rock fragments is on average only 2% of the detrital components. In addition, observed cherty grains are biogenic, not microcrystalline volcanic quartz [46]. The sandstone was interpreted to reflect initial transport from weathered (quartz-rich) silicate basement rocks and recurrent uplift and thrusting that caused a source change to recently developed carbonate platforms and older sedimentary basement [46].

Despite the low amount of sand-sized quartz, feldspar, and mica in rock fragments, the sandstone of Caja et al. [46] seems much more quartz-rich when using Gazzi–Dickinson-method categories for the proportions of quartz, feldspar, and lithic fragments as a base for diagrams than when using Indiana-method-based categories (Figure 4). The reason is that the high carbonate and polycrystalline-quartz content leads to an apparent composition with a majority of rock fragments when these components are included in the rock-fragment pool in accordance with the Indiana method (Figure 4). Comparison of the end members monocrystalline quartz, feldspar, and lithic fragments with polycrystalline quartz (cf. [1]) for Gazzi–Dickinson-counted data illustrates the full effect of only the carbonate clasts on the apparent composition (the remaining effect is due to the polycrystalline quartz; Figure 4).

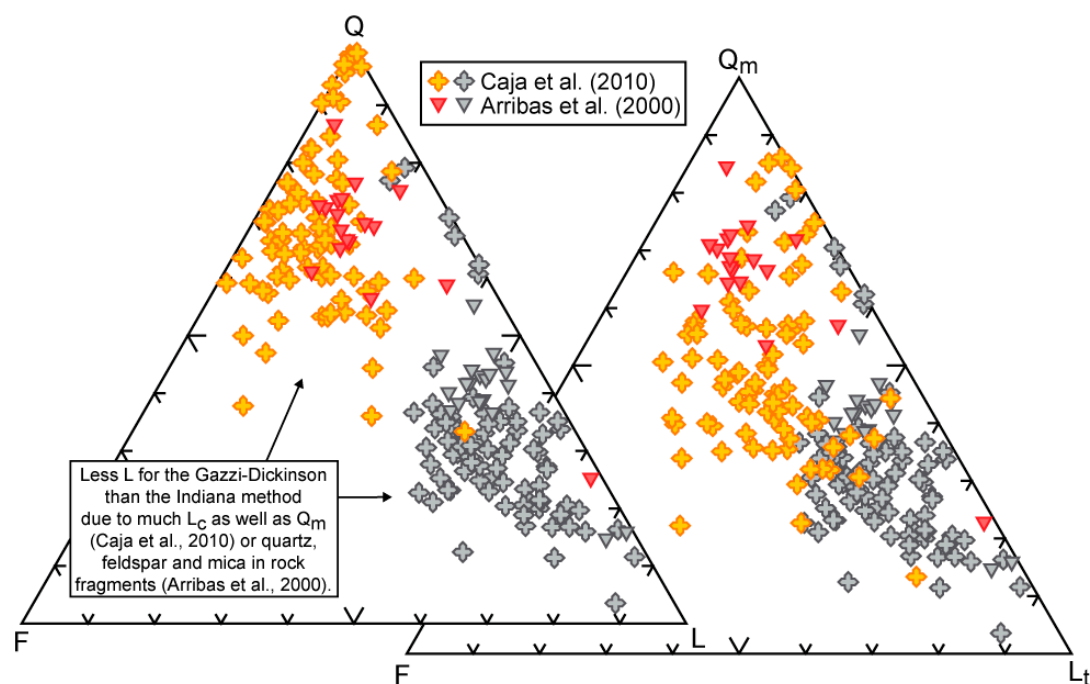


Figure 4. Apparent quartz-feldspar-lithic-fragment/rock-fragment (Q-F-L) composition difference for point-counting results based on the Gazzi–Dickinson (coloured symbols) and “pseudo”-Indiana (grey symbols) methods. Q includes

monocrystalline and polycrystalline quartz with chert for Gazzi–Dickinson-counted data, but only monocrystalline quartz for Indiana-method data. L only includes poly-mineralic grains for Gazzi–Dickinson data, but also carbonate and polycrystalline quartz (including chert) for Indiana-method data. For comparative reasons, the data also are shown with only monocrystalline quartz in the Q pool (Q_m) and all polycrystalline quartz in the L pool (L_t) (cf. [1]). The data for the “pseudo”-Indiana method is the same in both diagrams, as only monocrystalline quartz grains count as quartz. Clasts that were unspecified in the publications are included in the lithic-fragment pool (mostly 0–2% of the framework volume).

If the carbonate clasts are considered, their major abundance may give the illusion of a composition that is typical for transport from an igneous arc rather than a foreland-basin-related continent-collisional tectonic setting when provenance-discriminative diagrams that are not constructed for consideration of carbonate clasts are used (cf. Figure 1). In this case, such an interpretation should be easy to avoid, though, as arcs commonly rather contain igneous than carbonate rocks and cherty material of volcanic rather than sedimentary origin [1,73]. The carbonate-rich sandstone actually correctly mirrors the composition of mixed rifted shoulder—foreland-basin material from the warm and arid Arabian Peninsula [76]. If the carbonate clasts are not considered, though, an average of 35% of the framework composition is ignored. On the one hand, ignoring carbonate fragments would give the illusion of a rock composition that is more mature than in reality. On the other hand, the apparent composition also correctly would be in line with an association with uplifted foreland (recycled orogen and basement uplift in Dickinson and Suczek [1] and Dickinson et al. [2]). In addition, the mixed rift-foreland sand of Garzanti et al. [76] similarly is quartz-feldspar-rich. Hence, the high general content of carbonate clasts in the foreland-basin sandstone of Caja et al. [46] does not fully represent the assumed catchment area and rather masks the basin-external siliciclastic source types.

The story is partly different for recent fluvial sand from the Henares River in central Spain [47] that includes on average 11% carbonate clasts in the framework (equivalent to 40% of the total rock fragments). The amount of sand-sized quartz, feldspar, and mica crystals in rock fragments is 20%. The quartz fraction contains on average only 3% polycrystalline grains. The catchment area is mostly composed of metamorphic rocks, particularly in the upper part of the river system; carbonate rocks occur only to a minor degree in the catchment [47]. Thus, also in this study, the carbonate clasts are overrepresented.

Both the high carbonate content and the high amount of sand-sized quartz, feldspar, and mica in rock fragments in the Henares River study [47] cause a quartz-richer apparent composition for Gazzi–Dickinson-method than Indiana-method results (Figure 4). The low amount of polycrystalline quartz leads to a minor difference when only monocrystalline quartz (of Gazzi–Dickinson-method-based data) is part of the quartz pool (Figure 4). If a large amount of quartz, feldspar, and mica in rock fragments are treated as proper rock fragments in Gazzi–Dickinson-based discrimination schemes (because of the use of a different counting method), an arc-related depositional environment can falsely be assumed (Figures 1 and 4).

The two cases not only illustrate that apparent compositional differences based on the definition of the lithic/rock-fragment pool may be unrelated to geological processes but also the overrepresentation of carbonate clasts [46,47] illustrates that local erosion of chemically and mechanically unstable material can cause a source-unbalanced sediment composition. The exclusion of carbonate clasts for provenance interpretation may, in some cases, thus better represent the area of interest, but this provides that the extrabasinal part of the interior of the continental landmass is the main target of the study. Then, local carbonate contributions may be invisible in the data, although such information can lead to a more complete provenance interpretation (cf. [46]). In such cases, carbonate clasts may necessitate special attention because extrabasinal and intrabasinal carbonate components need to be differentiated for proper sediment-transport models (e.g., [75,77]).

3.5.3. Cases 3a and 3b—Apparent Compositional Bias: Chert

The continental to shallow-marine Triassic Barents Sea deposits of Mørk [33] contain more cherty grains in the Eastern than in the Western Barents Sea with mainly feldspatho-quartzose and litho-feldspatho-quartzose arenite (or subarkose and arkose) in the west and feldspatho-litho-quartzose, litho-feldspatho-quartzose and litho-quartzose arenite (or lithic arkose, lithic subarkose, and subarkose) in the east (Figure 2). The differences in chert abundance give the total sandstone set a larger apparent compositional spread in Garzanti's [23] than in McBride's [56] scheme (Figure 2). Therefore, optically also the compositional east-west difference seems to overlap less in Garzanti's [23] classification scheme. Based on the chert, other petrographic differences, heavy-mineral analysis, and garnet compositions, the deposits in the Eastern Barents Sea were concluded to be transported from the Uralides by Mørk [33], whereas the Western Barents Sea also includes Caledonian and other components [33]. Therefore, the large apparent compositional spread in the classification scheme of Garzanti [23] mirrors the provenance differences of the Barents Sea material better than the scheme of McBride [56].

Similar to the Barents Sea case, the also chert-rich (and carbonate-rich) Cretaceous gravity-flow sandstone from the Alps of von Eynatten and Gaupp [34] was interpreted to derive from two different sources. These were metamorphic and sedimentary, and both included carbonate, as well as ultramafic rocks and obducted oceanic crust. The source identifications were based on proportions of mafic minerals and rock-fragment components [34]. Neither of the petrographic classifications seem to obviously mirror two different source areas, despite the high content of cherty grains (Figure 2).

The two cases with chert illustrate the advantage of treating chert separately from other quartz components in some studies. They also demonstrate a common need for more specific rock-fragment investigations or other provenance methods.

4. Geological Bias

4.1. Sorting and Facies

Sediment sorting during transport is effective as soon as particles enter the transport system. Therefore, it is basically impossible to sample sedimentary material that represents the non-sorted composition of the detritus. Grus and material from local continental areas such as alluvial fans may be exceptions [13], but such deposits will give provenance information only on a local scale (e.g., [78–80]). Therefore, Ingersoll et al. [13] stressed that interpretations of the tectonic setting on a continental scale should be performed on “major river systems, deltas and submarine fans”. Thus, facies may affect what provenance signal is investigated, and comparison of petrographic results from different depositional settings, or sub-settings, may therefore artificially indicate different provenance (e.g., [11,81,82]).

Aeolian transport provides a larger density difference between the transport medium (air) and the transported material (sand grains) than for aqueous transport. Thus, grain-grain collisions will have a larger abrasional impact than in water, and this increases the plausibility for the formation of sub-sand-sized feldspar grains due to the low hardness (compared to quartz) and the cleavage planes of feldspar [83]. Similarly, Garzanti et al. [82] observed that heavy minerals are significantly abraded by air, but not by water, during coastal transport along the present-day Namib Desert. The study illustrates rapid compositional maturity for aeolian sand but insignificant compositional change after >1000 km of aqueous transport. A similar lack of mineralogical maturation during longshore transport has been observed for the light-mineral content of coastal sand [84]. Fluvial quartz-feldspar-rich sand also tends to be more feldspar-rich than littoral sand [25]. This is because in marine environments, the main break-up of feldspar and mechanically unstable rock fragments, including carbonate clasts, occurs along the coast (e.g., [85]). A similar trend has been observed for recent high-stand sand, whereby much of the increased maturity was explained by the abrasion of mechanically unstable volcanic lithic fragments [86]. Less difference in composition of fluvial and coastal low-stand sand was explained by sediment bypass [86]. Similarly, Critelli et al. [14] explained the observation that marine

mass-flow sand might have a mineralogically less mature composition than coastal sand with sediment bypassing the coastal area.

Grain-size and facies trends often appear together. In aeolian environments, selective entrainment of the small feldspar particles causes efficient mineral sorting [83], and therefore, aeolian feldspar grains may rather be of silt size, which can explain a low feldspar content for coarser material. Alternatively, Garzanti et al. [87] challenged the abrasional theory for diagenetic material and assumed that more feldspar is dissolved in high-permeable coarse-grained than in fine-grained sand, causing a compositional facies and grain-size trend. Nevertheless, numerous studies of Holocene fluvial sand have proven that the feldspar content often increases with decreasing grain size also without a diagenetic effect (e.g., [18,21,54,88]). Thus, the petrographic analysis of materials of different grain sizes in different samples, facies, regions, or stratigraphic positions may lead to erroneous provenance or climate interpretations that, in reality, are due to sorting effects (e.g., [81,89,90]). As an example, lithic to quartzo-lithic arenitic sand of the Waipaoa River system in New Zealand contains more feldspar and quartz (mostly monocrystalline grains) in the finest than in the coarsest sand fractions [29]. The lithic fragments are dominated by pelitic grains that were interpreted to be sourced from clay-mineral-rich rocks in the upper part of the catchment area. The feldspar and quartz grains in the fine fractions rather were assumed to derive from sandy deposits, thus postulating mixing between two sources of different lithology [29]. Hence, the grain-size trend was tied to sorting due to lithological variations in the catchment area.

4.2. *Compaction of Clay-Mineral-Rich Clasts*

The change in framework composition and texture that occurs during diagenesis of sandy deposits, including compaction of clay-mineral-rich clasts, may obscure the petrographic provenance signal (e.g., [91–93]). The differentiation between extrabasinal claystone (pelite) clasts and intrabasinal clay clasts is straightforward when pelite clasts are fairly round and similar in size to other detrital grains and when clay clasts are elongated and oversized (e.g., [94–96]). The difference in size and shape is due to the little compacted state of the low-density clay clasts, whereby the platy clay minerals lead to preferred crystal orientation, and the cohesive effect of them causes slow clast disintegration in flowing water (e.g., [94,96]). During mechanical compaction, the soft clay clasts commonly deform ductilely and are squeezed into intergranular pore spaces (e.g., [97]). Pelite clasts have a higher density and keep together more easily such that the grains can be transported longer distances, be abraded to a rounder shape than clay clasts, and be deposited together with similarly sized feldspar and quartz grains. During mechanical compaction, the rigid pelite clasts are fractured (e.g., [98]). However, similar to clay clasts, pelite clasts from poorly consolidated claystone—and clay-mineral-replaced feldspar and volcanic clasts—may compact ductilely and form a pseudomatrix that can be mistaken for a matrix or deformed intraclasts, and thus cause inappropriate provenance interpretations [53,91,93,99,100]. In line with this, Cox and Lowe [93] concluded that petrographic investigations for provenance research preferably should include all sandstone components, not only the detrital ones.

4.3. *Feldspar Dissolution and Replacement*

Feldspar, one of the main components in siliciclastic sandstone, is prone to dissolution or replacement during diagenesis, just like other chemically unstable components (e.g., finely crystalline lithic or rock fragments, mafic minerals, carbonate; e.g., [101–103]). The total amount of feldspar or fractions of different feldspar minerals in sandstone often is used in petrographic provenance studies (e.g., [1,26,104]). Nevertheless, their chemical instability commonly leads to dissolution, albitisation, or replacement by clay minerals, thus changing the petrographic provenance signal (e.g., [26,102,105]). Recalculation to the depositional framework composition may thus improve provenance interpretations. This can be done (1) based on geochemical mineral normalisations coupled to petrographic investigations of the same rocks [93], (2) by counting of all framework and diagenetic

components and textures [106], or (3) in addition by estimating both the present-day and original feldspar composition [102]. Based on optical observations, De Ros et al. [106] showed that present-day quartz-rich sandstone originally had higher feldspar contents due to secondary porosity, replaced grains, and diagenetic kaolinite that could be related to former feldspar. However, much feldspar dissolution may cause compaction of secondary pores during burial diagenesis without significant traces on a thin-section scale [101,107]. Furthermore, Wilkinson and Haszeldine [108] assumed, based on deeply buried sandstone from the North Sea, that aluminium is mobile during diagenesis such that observed kaolinite and illite contents only could explain a minor part of 30% reduction in feldspar content from 3.2 km to 4.5 km burial in their study. Thus, reconstructions may, in some cases, underestimate the original feldspar content, such that they rather represent minimum than absolute values [101,102,109]. Still, minimum feldspar values based on thorough observations of diagenetic features are valuable for provenance studies as they prove that quartz-richer original compositions are implausible.

Simplified reconstructions of original feldspar contents are here attempted based on the less detailed data available from the original publications in the data set. For a first recalculation (original composition I), all feldspar cement, kaolinite, and intragranular (or secondary) porosity are assumed to be formed from feldspar. The reason is that feldspar dissolution, for instance during near-surface diagenesis, may lead to the crystallisation of feldspar overgrowths, although feldspar cement tends to be a minor component volumetrically (e.g., [110,111]). It is more crucial that intragranular secondary porosity often can be tied to feldspar dissolution based on pore shapes or feldspar remnants (e.g., [102,103]). However, as petrographic estimations based only on the amount of secondary porosity tend to underestimate the original feldspar content [108], also kaolinite is included here. Kaolinite is a common product associated with feldspar dissolution, although it may form from mica as well [112], and although it does not necessarily crystallise in the space of the former feldspar grains. For a second recalculation (original composition II), all illite is additionally assumed ultimately to be formed due to feldspar dissolution. Illite often is a replacement product of potassium feldspar and kaolinite, or smectite [113,114], although it frequently also is detrital or possibly an altered infiltrated clay mineral (cf. [115–117]). This step is done to accommodate for cases where most illite ultimately resulted from feldspar dissolution.

The petrographic data of De Ros et al. [35] provide a quality check for the restoration methods as they recalculated the present-day quartzarenitic to subarkosic and sublitharenitic (or quartzose arenitic) composition of Silurian to Devonian fluvial sandstone in the Paraná Basin of Brazil to its plausible depositional composition. From their diagenetic study, they could differentiate kaolinitised feldspar from kaolinitised mica and pseudomatrix. They also observed signs of dissolved feldspar and illitised kaolinite and concluded that the sandstone originally was composed of 10–15% more feldspar in the framework and had a subarkosic composition. With the simplified recalculations, the same data indicate 10–30% more depositional feldspar than today and a subarkosic to quartz-rich arkosic (or feldspatho-quartzose arenitic) composition with original composition I. Original composition II indicate originally 20–30% more feldspar and feldspar-richer subarkose to arkose (or feldspar-richer feldspatho-quartzose arenite; Figure 5). The main reason is that the Silurian–Devonian sandstone partly has undergone much kaolinitisation of mica and pseudomatrix (sometimes 10–20%), and in other places, it is strongly affected by illitisation of pseudomatrix (sometimes approximately 10%). Therefore, recalculations I and II give larger original compositional ranges than the recalculations of De Ros et al. [35], sometimes even pointing to a less feldspar-rich composition than in the original publication. Thus, the simplified recalculations particularly are applicable for studies that do not track all provenance-relevant diagenetic processes. Then, sandstone samples should be treated as a group rather than individually, as the individual data may spread significantly.

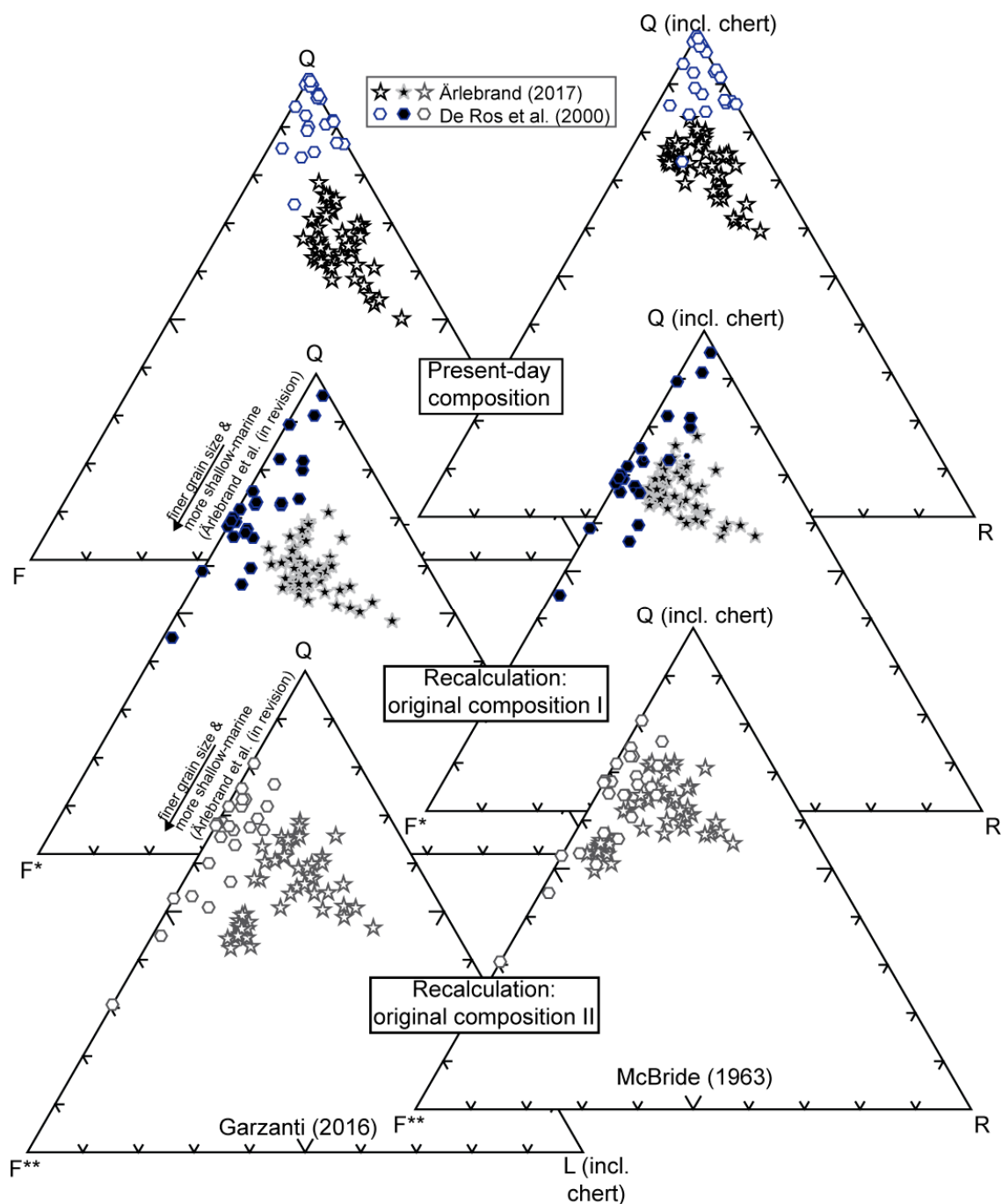


Figure 5. Comparison between present and estimated original compositions in Garzanti's [23] (left) and McBride's [56] (right) classification schemes, but without discrimination lines. Carbonate clasts are included in the lithic-fragment/rock-fragment pool in both cases. * Original composition I includes detrital feldspar, as well as feldspar cement, kaolinite, and intragranular/secondary porosity in the feldspar pool. ** Original composition II includes detrital feldspar, as well as feldspar cement, kaolinite, illite, and intragranular/secondary porosity in the feldspar pool. F: feldspar; L: lithic fragments; Q: quartz (both monocrystalline and polycrystalline grains); R: rock fragments.

4.4. Cases Studies on Geological Bias

4.4.1. Cases 4a, 4b and 4c—Compaction and Dissolution

The Cretaceous alluvial-fluvial sandstone of Caja Rodríguez [45] mainly is feldspatho-quartzose and litho-feldspatho-quartzose arenite (or subarkose and lithic subarkose; Figure 2). Rock fragments compose up to approximately 20% of the framework, and these clasts are dominated by pseudomatrix. Photographic images illustrate compacted, plastically

deformed material that has filled the interstices between more competent material; the original grain size and shape are destroyed due to the deformation. The pseudomatrix was stated to originate from metasedimentary rock fragments [45], possibly because it contains microscopic mica crystals. With an estimated maximum burial temperature of 65 °C, the pseudomatrix also could be differentiated from soft clay intraclasts [45], which commonly is observed in fluvial deposits. Thus, a detrital origin indeed is plausible for the pseudomatrix. Therefore, all rock fragments (except for very few carbonate grains) are of metamorphic or plutonic origin [45].

Without diagenetic investigations of the rocks, sericite in pseudomatrix potentially may lead to the assumption of diagenetically formed mica and that the pseudomatrix were of sedimentary origin (cf. [99,118,119]). This would cause the illusion of dominance of sedimentary (Figure 6) instead of metamorphic clasts in the Cretaceous sandstone of Caja Rodríguez [45]. In addition, a misinterpretation of the pseudomatrix as proper matrix or intraclasts in the Cretaceous study would lead to an illusive larger influence of igneous material in the sandstone as many rock fragments then would seem to be of plutonic origin (Figure 6).

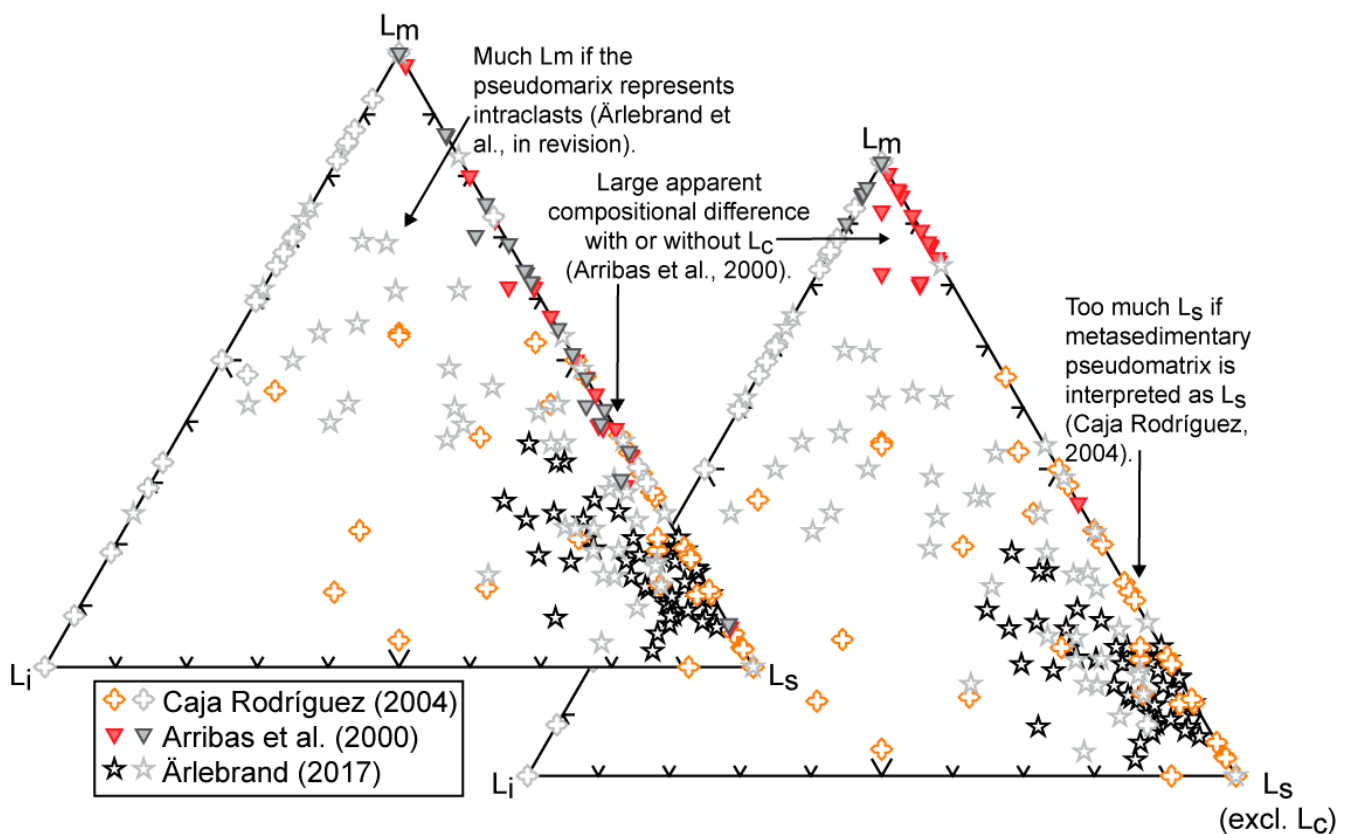


Figure 6. Effect of different interpretations of clay-mineral-rich clasts and pseudomatrix. The coloured symbols represent a composition where all clasts that have been interpreted as pelite clasts and pseudomatrix are assumed to be true pelite clasts. The grey symbols are compositions without pelite clasts, assuming that they represent intrabasinal clay clasts. Crystals of quartz, feldspar, and mica that were counted separately with the Gazzi–Dickinson method in Arribas et al. [47] were assigned to L_m as specified in the original publication. Caja Rodríguez [45] applied the Indiana point-counting method, and Årlebrand [40] used the Gazzi–Dickinson method with a 20 μm grain-matrix limit without specifying the rock-fragment types that single sand-sized crystals were part of. Cherty grains (microcrystalline quartz) are not included in the diagrams as they potentially may be either of sedimentary or volcanic origin. The diagrams are based on total average amounts of 91, 37, and 34 grains per sample for Arribas et al. [47], Caja Rodríguez [45], and Årlebrand [40], respectively. L: lithic fragments; L_c : carbonate L; L_i : igneous L (both plutonic and volcanic grains); L_m : metamorphic L; L_s : sedimentary L.

The recent sand from the Henares River in central Spain of Arribas et al. [47] is composed mainly of feldspatho-litho-quartzose arenite (or litharenite and feldspathic litharenite; Figure 2). Rock fragments represent >40% of the framework (15–25% lithic fragments with the Gazzi–Dickinson method). The rock-fragment fraction is dominated by sedimentary and metamorphic clasts; very few igneous (in this case: volcanic) grains were reported (Figure 6). The sedimentary rock-fragment population is dominated by carbonate clasts, and clay-mineral-rich clasts are represented by shale fragments [47].

If the shale fragments incorrectly would have been identified as intraclasts (for instance, in similar but mechanically more compacted deposits than in the study of Arribas et al. [47]), the ratio between metamorphic and sedimentary clasts would increase only slightly. Nevertheless, carbonate clasts may dissolve and further reduce the amount of detrital sedimentary rock fragments. Thus, with compaction of the shale clasts and dissolution of the carbonate grains in the Henares River sand, the deposits would seem to lack sedimentary rock fragments, and solely metamorphic source areas would be assumed (Figure 6). Hence, these two hypothetical cases illustrate how compaction and carbonate dissolution may lead to either an overestimation or an underestimation of sedimentary and other clast types.

Compositionally different, the mineralogically mature sandstone of Lorentzen et al. [42,43] from the Cambrian of Scandinavian Baltica provides samples mostly with quartzarenite (or pure quartzose arenite [59]). The sandstone contains on average 20% quartz cement, 3% illite, and 1% kaolinite of the total rock volume [42,43]. In addition, a dominance of concave-convex grain-grain contacts, abundant stylolites, and some ductilely deformed grains were observed. Porosity is mostly absent, but rare intragranular pores were detected. The kaolinite was suggested to be eodiagenetic at shallow depths [42], and consequently, some feldspar reduction was interpreted to be due to kaolinitisation and chemical compaction, although most sand maturation was assumed to have taken place already during sediment reworking [42,43]. In addition, the illite partly was interpreted as a product of the reaction between feldspar and kaolinite during burial. The near absence of intragranular pores potentially may partly be due to compaction of secondary pores and export of dissolved aluminium in an open diagenetic system. Recalculation to original composition II leads to subarkosic to quartzarenitic (or feldspatho-quartzose to quartzose arenitic) original compositions (not illustrated in this contribution) that may indicate a former higher original feldspar content in line with the diagenetic features.

4.4.2. Case 5—Facies vs. Climate

Lippmann [36] provided petrographic data that represent a transition from Permian and Triassic continental to Jurassic and Palaeocene marine deposits in the North Sea. The climate evolved, with some smaller-scale fluctuations, from arid conditions during Permian and Triassic time [120,121] to higher humidity during Jurassic and Palaeocene time [122,123]. The North Sea study was diagenetic, so the sediment-transport routes were not reconstructed. Still, the location of the studied wells in the Central Graben allows for Permian to Jurassic and Palaeocene sediment transport directly or as sedimentary recycled material from the Scandinavian and British Caledonides, although the provenance partly is poorly constrained (e.g., [124–126]).

The deposits are mostly feldspatho-quartzose and quartzose arenite (or arkose, subarkose and quartzarenite; Figure 2). A grain-size trend seems absent, but Permo–Triassic continental, mostly fluvial, deposits are rather feldspar-rich with 20–60% feldspar in the framework. Differently, post-Triassic marine, mostly shoreface, deposits are composed of <20% feldspar (Figure 7). No difference was detected in the amount of lithic/rock fragments (<15% of the framework). A low number of counted lithic/rock fragments (on average eight grains per sample) does not allow for a provenance-relevant differentiation of them.

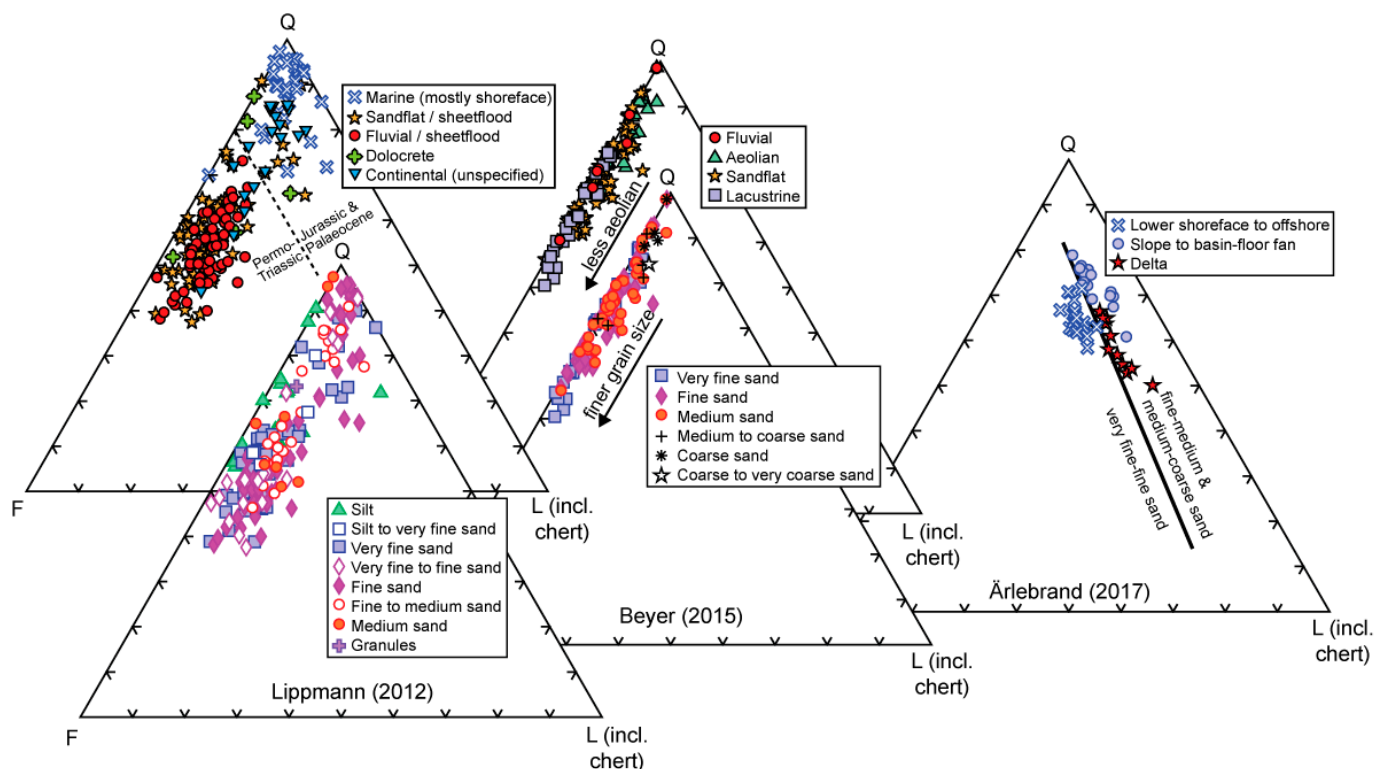


Figure 7. Grain-size sorting in relation to facies in Gazzi–Dickinson-based compositional diagrams that exclude carbonate clasts. The data of Årlebrand [40] were counted using the Gazzi–Dickinson method but with a 20 μm grain-matrix size limit. Lippmann [36] and Beyer [39] did not mention the used counting method. Few samples with the vague grain-size specification “sand” [36,39] are not plotted in the grain-size figures. F: feldspar; L: lithic/rock fragments; Q: quartz (both monocrystalline and polycrystalline grains).

The higher mineralogical maturity of the shoreface than fluvial deposits is in line with the expected difference between fluvial and littoral sand or sandstone due to break-up of feldspar and other mechanically unstable grains in the coastal realm before further marine transport that is rather unlikely to modify the composition much (e.g., [25,82,85]). However, the compositional trend also reflects the climate change from arid to humid conditions. The compositional evolution thus possibly illustrates both a facies shift towards shoreface settings and towards more humid conditions. The difference between mineralogically immature fluvial sandstone and mature shoreface sandstone is actually similar to the difference between fluvial sand of plutonic detritus in arid and humid areas, as shown by Suttner et al. [21], although it is unclear if comparable counting methods have been used. Thus, in this case, the effects of sorting and climate on the petrographic composition cannot be differentiated.

4.4.3. Case 6—Sorting and Feldspar Dissolution vs. Provenance

The diagenetic studies of Weibel and Friis [38], Beyer [39], and Olivarius et al. [37] provide petrographic data from continental Triassic sandstone in Denmark and Germany. At the time, the area of deposition, the Central European Basin, is estimated to have been arid with supermonsoons and with a transition to sub-humid conditions during the late Olenekian [127]. Mostly, the sandstone represents feldspatho-quartzose arenitic (or subarkosic to arkosic) compositions. Only the data of Beyer [39] from Germany illustrate a minor grain-size trend with the highest feldspar contents for the finest sand sizes and with a facies trend with less feldspar in aeolian than lacustrine sandstone; sandflat deposits bridge the two end-members (Figure 7). Beyer’s [39] data from approximately 450–900 m depth in well Rockensußra 2/83, Germany, illustrated similar grain-size and facies trends for feldspar as his complete data set (Figure 3). In addition, aeolian sandstone has the

highest lithic/rock-fragment contents (for samples in which such grains were identified) and the lowest contents of monocrystalline quartz in the quartz fraction (Figure 3). The aeolian sandstone is coarser-grained than the lacustrine sandstone (Figure 3). Thus, both grain-size and facies trends are present. Irrespective of facies and grain size, the proportions of monocrystalline quartz increase up-section from sandstone deposited in arid conditions to sandstone from sub-humid climate, and the feldspar content increases with depth (Figure 3).

Time-equivalent sandstone from south-westernmost Jutland in Denmark [37,38] neither reveals a grain-size nor a facies trend, but the sandstone above 1700 m is richer in feldspar and lithic/rock fragments than below 1700 m, irrespective of the geological unit and facies (Figure 8). Similar to the German sandstone, the amount of monocrystalline quartz grains in the quartz fraction seems higher in the youngest unit, but the data are too scarce for a high-probability statement (Figure 8).

The higher feldspar content for lacustrine and finest-grained sandstone than aeolian and coarser sandstone in Germany is in line with mineral sorting and most feldspar abrasion in aeolian environments. In the deeper Danish wells, the lack of a similar trend may be due to feldspar and lithic/rock-fragment dissolution, as indicated by the decreasing trends with depth for such components. It also indicates that the climate change from arid to more humid in the upper section is not detected in the feldspar and rock-fragment contents.

The low amount of monocrystalline quartz in aeolian sandstone theoretically may be due to several reasons: (1) Mechanical and chemical abrasion of quartz grains and quartz-prone lithic fragments during weathering and transport can lead to the break-up of large grains along crystal boundaries with an increase in monocrystalline grains the finer-grained the material is [7,54,85,88]. The data support this as the aeolian deposits in general are coarser-grained than the aqueous sandstone and also has the lowest relative amounts of monocrystalline grains. (2) Transport from different source rocks may also lead to the preferential formation of sand grains of monocrystalline or polycrystalline quartz. This would assume that the quartz types illustrate a slight shift in provenance. The source-rock explanation is in line with a suggested provenance trend of Olivarius et al. [128] that is based on ages of detrital zircon grains. Therefore, a sorting effect cannot be differentiated from a provenance effect for the quartz proportions alone in this case.

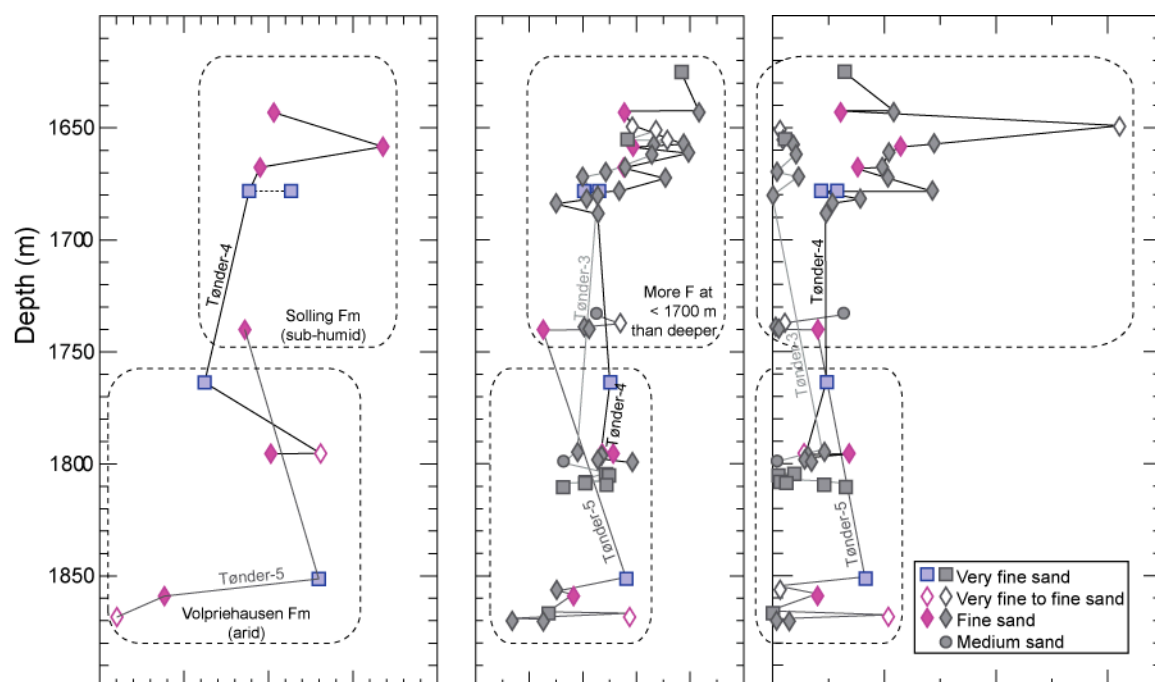


Figure 8. Cont.

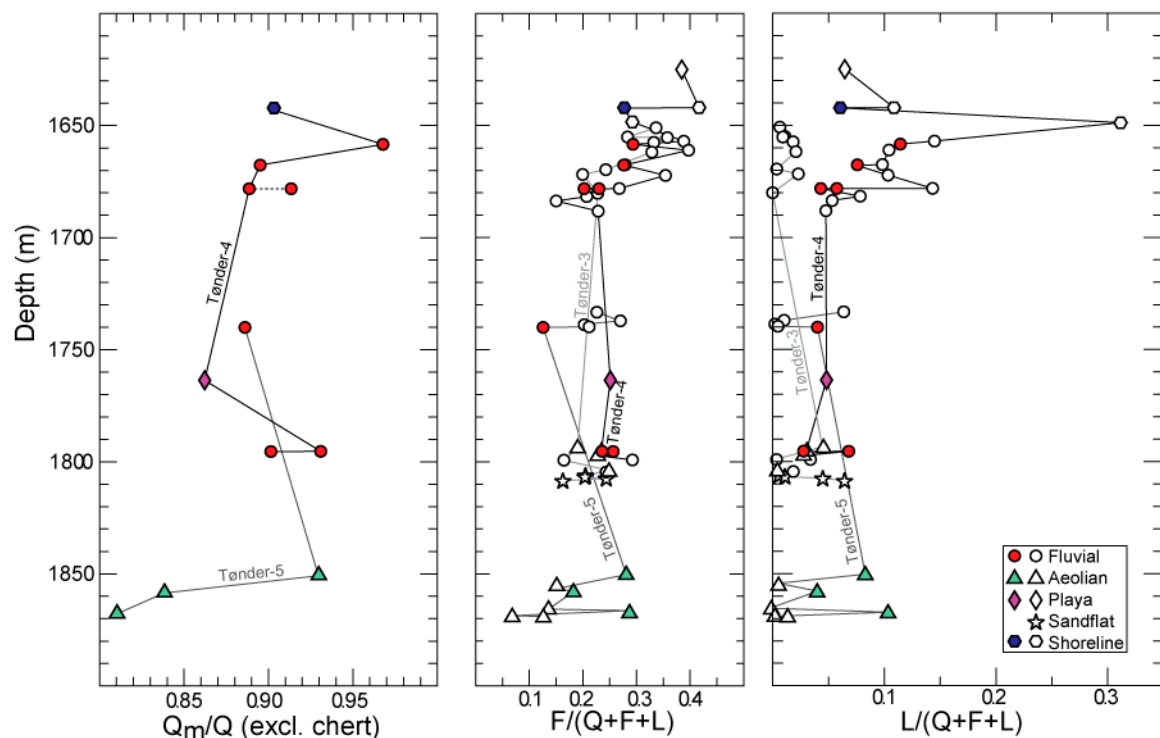


Figure 8. Grain-size and facies compositional trends for Early Triassic sandstone in wells Tønder-3, Tønder-4, and Tønder 5 (Denmark) based on data from Weibel and Friis [38] (coloured symbols) and Olivarius et al. [37] (white and grey symbols). Samples from the same depth are connected with dotted lines (best visible in the left-most diagrams). Samples from both studies were used together to evaluate compositional trends as care was taken to make the results from the two operators coherent [129]. Among the few rock fragments, sedimentary and plutonic or unspecified igneous grains dominate [37,38]. F: feldspar; L: lithic/rock fragments (poly-mineralic grains only; no carbonate clasts were detected); Q: quartz (both monocrystalline and polycrystalline grains); Q_m : monocrystalline Q.

4.4.4. Cases 7—Facies vs. Diagenesis vs. Tectonic Setting

The Cretaceous Barents Sea sandstone of Ärlebrand [40] is dominated by litho-quartzose to feldspatho-litho-quartzose arenite (or sublitharenite to lithic subarkose) with up to 15% lithic fragments. Very fine sandstone is more feldspar-rich than coarser sandstone (Figure 7). Independent of the grain size, also a marine facies trend is present with more lithic fragments in deltaic sandstone than in slope-to-basin-floor deposits of plausibly the same sedimentary system (Figure 7). Thus, the facies trend indicates a reduction in lithic-fragment content from shallow to deep areas (Figure 7). Most lithic fragments were interpreted as pelite clasts, including pseudomatrix. Ärlebrand [40] defined pseudomatrix as deformed clay-mineral-rich material in a restricted area on a thin-section level (secondary matrix to pseudomatrix as defined by Valloni et al. [99]). Its origin was interpreted as mudstone clasts, and other clay-mineral-rich material was considered as matrix. The pseudomatrix was illustrated as a clay-mineral-rich mass that plastically has engulfed more competent material [40]. The pseudomatrix dominates in the pelite-clast pool.

The facies and grain-size trends partly prevail after recalculations to original depositions I and II (Figure 5). Therefore, the grain-size trend may at first glance seem to be due to sorting, but Ärlebrand [40] interpreted it to reflect true provenance variations based on different amounts of chert and pelite clasts. Nevertheless, if the pseudomatrix (that is included in the pelite fraction) in reality represents deformed and ductile intrabasinal clay clasts, the deposits are dominated by metamorphic rather than sedimentary clasts (Figure 6). This has the potential to change both the source-rock and sediment-transport interpretation. Assuming correct classification of the pseudomatrix, the maturity difference between mass-flow and deltaic sandstone can be explained by the tectonic surroundings because a fault complex is situated between the proposed source area and the depositional

basin [130]. Faulting may either imply too short a time scale for sediment transport from source to sink for maturation in the coastal area for the deltaic deposits (cf. [11]), or that the mass-flow deposits were affected by abrading wave action during coastal reworking before their final deposition in deeper water. Then, the deltaic sandstone was mostly exposed to less abrasive currents in the fluvial system. Hence, an interplay between tectonic processes and sorting may explain the differences observed for the deltaic and mass-flow deposits.

5. Conclusions and Recommendations

The cases that illustrate geological and non-geological biases that may affect provenance interpretations lead to these conclusions and recommendations for petrographic investigations of sand and sandstone:

Data from different operators should not be compared directly unless their operator bias is coherent and standardised. Instead, only one operator should count all samples in single studies, or several operators should count all samples.

It is recommended to use a point-counting method that is appropriate for the goal of the study. Alternatively, the use of enough compositional and textural categories to allow for recalculation between different counting methods gives large flexibility for the presentation of petrographic data.

Only diagrams that are constructed for the applied counting method should be used. This is particularly relevant for diagrams with discriminative lines, including sandstone-classification diagrams that have been defined on a set of data that was produced with a specific counting method. Preferably, the counting method and matrix-size cut-off should be specified, or described, in the study.

Sub-groups of rock fragments give more specific provenance information than the relative amounts of quartz, feldspar, and lithic/rock fragments. However, compositional diagrams, with or without discriminative fields, should be chosen such that the uncertainty for the result is small; hence, the number of counts for the included categories should be high. Therefore, a separate count only for rock fragments may be needed for sandstone with a low content of rock fragments in order to quantify sub-groups of them.

Misinterpretation of pseudomatrix as intraclasts or rock fragments may lead to underestimation or overestimation of the original rock-fragment content. Similarly, incorrect interpretation of the origin of rock fragments or detrital pseudomatrix (most likely sedimentary vs. volcanic vs. metasedimentary origins) may lead to incorrect provenance assumptions.

Absolute source indications based on the petrographic composition of sandstone may improve by estimations of the depositional composition from diagenetic features. This can be done by recalculations after interpretation of the diagenetic processes that have affected the sandstone composition.

Finally, the comparison of material of similar grain size and facies may be advantageous to avoid sorting and facies bias. Stratigraphic visualisation of compositional data may aid the quantification of bias, including diagenesis, as well as identifying probable compositional variations due to climate and provenance changes. Thus, all extrabasinal and intrabasinal processes that are relevant for a provenance study should be considered.

Supplementary Materials: The following are available online at <https://www.mdpi.com/article/10.3390/geosciences11050205/s1>, Table S1: petrographic data.

Funding: This research received no external funding.

Acknowledgments: Thanks to Abhijit Basu for fruitful discussions regarding the Indiana method and to Luca Caracciolo for discussions and comments on earlier versions of this paper. Comments that led to the improvement of this contribution from three anonymous reviewers and the guest editors Emilia Le Pera and Consuele Morrone also were appreciated.

Conflicts of Interest: The author declares no conflict of interest.

References

1. Dickinson, W.R.; Suczek, C.A. Plate Tectonics and sandstone compositions. *Am. Assoc. Pet. Geol. Bull.* **1979**, *63*, 2164–2182.
2. Dickinson, W.R.; Beard, L.S.; Brakenridge, G.R.; Erjavec, J.L.; Ferguson, R.C.; Inman, K.F.; Knepp, R.A.; Lindberg, F.A.; Ryberg, P.T. Provenance of North American Phanerozoic sandstones in relation to tectonic setting. *Geol. Soc. Am. Bull.* **1983**, *94*, 222–235. [[CrossRef](#)]
3. Weltje, G.J. Ternary sandstone composition and provenance: An evaluation of the ‘Dickinson model’. In *Compositional Data Analysis in the Geosciences: From Theory to Practice*; Buccianti, A., Mateu-Figueras, G., Pawlowsky-Glahn, V., Eds.; Geological Society: London, UK, 2006; pp. 79–99.
4. Potter, P.E. Modern sands of South America: Composition, provenance and global significance. *Geol. Rundsch.* **1994**, *83*, 212–232. [[CrossRef](#)]
5. Critelli, S. Provenance of Mesozoic to Cenozoic circum-Mediterranean sandstones in relation to tectonic setting. *Earth Sci. Rev.* **2018**, *185*, 624–648. [[CrossRef](#)]
6. Suttner, L.J.; Dutta, P.K. Alluvial sandstone composition and paleoclimate, I. Framework mineralogy. *J. Sediment. Petrol.* **1986**, *56*, 329–345.
7. Johnsson, M.J.; Stallard, R.F.; Meade, R.H. First-cycle quartz arenites in the Orinoco river basin, Venezuela and Colombia. *J. Geol.* **1988**, *96*, 263–277. [[CrossRef](#)]
8. Hessler, A.M.; Lowe, D.R. Initial generation of sand across climate zones of the Mojave, Sierra Nevada, and Klamath Batholiths in California, U.S.A. *Sediment. Geol.* **2017**, *348*, 37–50. [[CrossRef](#)]
9. Garzanti, E.; He, J.; Barbarano, M.; Resentini, A.; Li, C.; Yang, L.; Yang, S.; Wang, H. Provenance versus weathering control on sediment composition in tropical monsoonal climate (South China)—2. Sand petrology and heavy minerals. *Chem. Geol.* **2021**, *564*, 119997. [[CrossRef](#)]
10. Johnsson, M.J. The System Controlling the Composition of Clastic Sediments. In *Processes Controlling the Composition of Clastic Sediments*; Geological Society of America: Washington, DC, USA, 1993; pp. 1–19.
11. Caracciolo, L. Provenance analysis perspective: Review, application and future development. *Earth Sci. Rev.* **2020**, *209*, 103226. [[CrossRef](#)]
12. Garzanti, E.; Dinis, P.; Vermeesch, P.; Andò, S.; Hahn, A.; Huvi, J.; Limonta, M.; Padoan, M.; Resentini, A.; Rittner, M.; et al. Dynamic uplift, recycling, and climate control on the petrology of passive-margin sand (Angola). *Sediment. Geol.* **2018**, *375*, 86–104. [[CrossRef](#)]
13. Ingersoll, R.V.; Kretchmer, A.G.; Valles, P.K. The effect of sampling scale on actualistic sandstone petrofacies. *Sedimentology* **1993**, *40*, 937–953. [[CrossRef](#)]
14. Critelli, S.; Le Pera, E.; Ingersoll, R.V. The effects of source lithology, transport, deposition and sampling scale on the composition of southern California sand. *Sedimentology* **1997**, *44*, 653–671. [[CrossRef](#)]
15. Lawrence, R.L.; Cox, R.; Mapes, R.W.; Coleman, D.S. Hydrodynamic fractionation of zircon age populations. *Geol. Soc. Am. Bull.* **2011**, *123*, 295–305. [[CrossRef](#)]
16. Malusà, M.G.; Carter, A.; Limoncelli, M.; Villa, I.M.; Garzanti, E. Bias in detrital zircon geochronology and thermochronometry. *Chem. Geol.* **2013**, *359*, 90–107. [[CrossRef](#)]
17. Ibañez-Mejía, M.; Pullen, A.; Pepper, M.; Urbani, F.; Ghoshal, G.; Iañez-Mejía, J.C. Use and abuse of detrital zircon U-Pb geochronology—A case from the Río Orinoco delta, eastern Venezuela. *Geology* **2018**, *46*, 1019–1022. [[CrossRef](#)]
18. Ingersoll, R.V.; Bullard, T.R.; Ford, R.L.; Grimm, J.P.; Pickle, J.D.; Sares, S.W. The effect of grain size on detrital modes: A test of the Gazzi-Dickinson point-counting method. *J. Sediment. Petrol.* **1984**, *54*, 103–116.
19. Garzanti, E.; Vezzoli, G. A classification of metamorphic grains in sands based on their composition and grade. *J. Sediment. Res.* **2003**, *73*, 830–837. [[CrossRef](#)]
20. Augustsson, C.; Aehnelt, M.; Voigt, T.; Kunkel, C.; Meyer, M.; Schellhorn, F. Quartz and zircon de-coupling in sandstone: Petrography and quartz cathodoluminescence of the Early Triassic continental Buntsandstein Group in Germany. *Sedimentology* **2019**, *66*, 2874–2893. [[CrossRef](#)]
21. Suttner, L.J.; Basu, A.; Mack, G.H. Climate and the origin of quartz arenites. *J. Sediment. Petrol.* **1981**, *51*, 1235–1246.
22. Johnsson, M.J. Tectonic versus chemical-weathering controls on the composition of fluvial sands in tropical environments. *Sedimentology* **1990**, *37*, 713–726. [[CrossRef](#)]
23. Garzanti, E. From static to dynamic provenance analysis—Sedimentary petrology upgraded. *Sediment. Geol.* **2016**, *336*, 3–13. [[CrossRef](#)]
24. Suttner, L.J. Sedimentary petrographic provinces: An evaluation. *Soc. Econ. Paleontol. Mineral. Spec. Publ.* **1974**, *21*, 75–84.
25. Mack, G.H. The survivability of labile light-mineral grains in fluvial, aeolian and littoral marine environments: The Permian Cutler and Cedar Mesa Formations, Moab, Utah. *Sedimentology* **1978**, *25*, 587–604. [[CrossRef](#)]
26. Helmold, K.P. Provenance of feldspathic sandstones—The effect of diagenesis on provenance interpretations: A review. In *Provenance of Arenites*; Zuffa, G.G., Ed.; Springer: Dordrecht, The Netherlands, 1985; pp. 139–163.
27. Garzanti, E. Source rock versus sedimentary control on the mineralogy of deltaic volcanic arenites (Upper Triassic, northern Italy). *J. Sediment. Petrol.* **1986**, *56*, 267–275.

28. Cavazza, E.; Zuffa, G.G.; Camporesi, C.; Ferretti, C. Sedimentary recycling in a temperate climate drainage basin (Senio River, north-central Italy): Composition of source rock, soil profiles, and fluvial deposits. In *Processes Controlling the Composition of Clastic Sediments*; Johnsson, M.J., Basu, A., Eds.; Special Papers-Geological Society of America: Washington, DC, USA, 1993; pp. 247–261.
29. James, D.E.; DeVaughn, A.M.; Marsaglia, K.M. Sand and gravel provenance in the Waipaoa River system: Sedimentary recycling in an actively deforming forearc basin, North Island, New Zealand. In *Sedimentary Provenance and Petrogenesis: Perspectives from Petrography and Geochemistry*; Arribas, J., Critelli, S., Johnsson, M.J., Eds.; Special Papers-Geological Society of America: Washington, DC, USA, 2007; pp. 253–276.
30. Bangs Rooney, C.; Basu, A. Provenance analysis of muddy sandstones. *J. Sediment. Res.* **1994**, *64*, 2–7.
31. Nirasawa, M.; Minato, Y.; Yagishita, K. Two point-counting methods for modal analyses of Holocene sands: Their comparison and evaluation. *J. Sediment. Soc. Jpn.* **1998**, *48*, 85–93. [[CrossRef](#)]
32. Götze, J. Geochemistry and provenance of the Altendorf feldspathic sandstone in the Middle Bunter of the Thuringian basin (Germany). *Chem. Geol.* **1998**, *150*, 43–61. [[CrossRef](#)]
33. Mørk, M.B.E. Compositional variations and provenance of Triassic sandstones from the Barents Shelf. *J. Sediment. Res.* **1999**, *69*, 690–710. [[CrossRef](#)]
34. von Eynatten, H.; Gaupp, R. Provenance of Cretaceous synorogenic sandstones in the Eastern Alps: Constraints from framework petrography, heavy mineral analysis and mineral chemistry. *Sediment. Geol.* **1999**, *124*, 81–111. [[CrossRef](#)]
35. De Ros, L.F.; Morad, S.; Broman, C.; De Césero, P.; Gomez-Gras, D. Influence of uplift and magmatism on distribution of quartz and illite cementation: Evidence from Siluro-Devonian sandstones of the Paraná Basin, Brazil. *Spec. Publ. Int. Assoc. Sediment.* **2000**, *29*, 231–252.
36. Lippmann, R. Diagenesis in Rotliegend, Triassic and Jurassic Clastic Hydrocarbon Reservoirs of the Central Graben, North Sea. Ph.D. Thesis, Friedrich Schiller University Jena, Jena, Germany, 2012.
37. Olivarius, M.; Weibel, R.; Hjuler, M.L.; Kristensen, L.; Mathiesen, A.; Nielsen, L.H.; Kjøller, C. Diagenetic effects on porosity-permeability relationships in red beds of the Lower Triassic Bunter Sandstone Formation in the North German Basin. *Sediment. Geol.* **2015**, *321*, 139–153. [[CrossRef](#)]
38. Weibel, R.; Friis, H. Opaque minerals as keys for distinguishing oxidising and reducing diagenetic conditions in the Lower Triassic Bunter Sandstone, North German Basin. *Sediment. Geol.* **2004**, *169*, 129–149. [[CrossRef](#)]
39. Beyer, D. Evolution of Reservoir Properties in the Lower Triassic Aquifer Sandstones of the Thuringian Syncline in Central Germany. Ph.D. Thesis, Friedrich Schiller University Jena, Jena, Germany, 2015.
40. Årlebrand, A. Depositional Setting and Diagenesis as Keys to Reservoir Quality: Lower Cretaceous in the Southwestern Barents Sea. Master's Thesis, University of Stavanger, Stavanger, Norway, 2017.
41. Lorentzen, S. Global vs. Local Factors for the High Sediment Maturity of Cambrian Quartz Sandstone. Ph.D. Thesis, University of Stavanger, Stavanger, Norway, 2019.
42. Lorentzen, S.; Augustsson, C.; Jahren, J.; Nystuen, J.P.; Schovsbo, N.H. Tectonic, sedimentary and diagenetic controls on sediment maturity of lower Cambrian quartz arenite from southwestern Baltica. *Basin Res.* **2019**, *31*, 1098–1120. [[CrossRef](#)]
43. Lorentzen, S.; Braut, T.; Augustsson, C.; Nystuen, J.P.; Jahren, J.; Schovsbo, N.H. Provenance of lower Cambrian quartz arenite on southwestern Baltica: Weathering versus recycling. *J. Sediment. Res.* **2020**, *90*, 493–512. [[CrossRef](#)]
44. von Eynatten, H. Provenanzanalyse kretazischer Siliziklastika aus den Nördlichen Kalkalpen. Petrographie, Mineralchemie und Geochronologie des frühalpindisch umgelagerten Detritus. Ph.D. Thesis, Johannes Gutenberg-Universität Mainz, Mainz, Germany, 1996.
45. Caja Rodríguez. Procedencia y Diagénesis de los Sedimentos del Jurásico Superior-Cretácico Inferior (facies Weald) en las Subcuencas Occidentales de la Cuenca del Maestrazgo, Cordillera Ibérica Oriental. Ph.D. Thesis, Universidad Complutense de Madrid, Madrid, Spain, 2004.
46. Caja, A.; Marfil, R.; Garcia, D.; Remacha, E.; Morad, S.; Mansurbeg, H.; Amorosi, A.; Martínez-Calvo, C.; Lahoz-Beltrá, R. Provenance of siliciclastic and hybrid turbiditic arenites of the Eocene Hecho Group, Spanish Pyrenees: Implications for the tectonic evolution of a foreland basin. *Basin Res.* **2010**, *22*, 157–180. [[CrossRef](#)]
47. Arribas, J.; Critelli, S.; Le Pera, E.; Tortosa, A. Composition of modern stream sand derived from a mixture of sedimentary and metamorphic source rocks (Henares River, Central Spain). *Sediment. Geol.* **2000**, *133*, 27–48. [[CrossRef](#)]
48. Wentworth, C.K. A scale of grade and class terms for clastic sediments. *J. Geol.* **1922**, *30*, 377–392.
49. Powers, M.C. A new roundness scale for sedimentary particles. *J. Sediment. Petrol.* **1953**, *23*, 117–119. [[CrossRef](#)]
50. Folk, R.L.; Ward, W.C. Brazos River bar: A study in the significance of grain size parameters. *J. Sediment. Petrol.* **1957**, *27*, 3–26. [[CrossRef](#)]
51. Krumbein, W.C.; Sloss, L.L. *Stratigraphy and Sedimentation*, 2nd ed.; Freeman and Company: San Francisco, CA, USA, 1963; p. 660.
52. Longiaru, S. Visual comparators for estimating the degree of sorting from plane and thin section. *J. Sediment. Petrol.* **1987**, *57*, 791–794. [[CrossRef](#)]
53. Dickinson, W.R. Interpreting detrital modes of graywacke and arkose. *J. Sediment. Petrol.* **1970**, *40*, 695–707.
54. Basu, A. Petrology of Holocene fluvial sand derived from plutonic source rocks: Implications to paleoclimatic interpretation. *J. Sediment. Petrol.* **1976**, *46*, 694–709.
55. Basu, A. (Indiana University, Bloomington, IN, USA). Personal communication, 2021.
56. McBride, E. A classification of common sandstones. *J. Sediment. Petrol.* **1963**, *33*, 664–669.

57. Demirmen, F. Counting error in petrographic point-count analysis: A theoretical and experimental study. *Math. Geol.* **1971**, *3*, 15–41. [[CrossRef](#)]
58. Weltje, G.J. Quantitative analysis of detrital modes: Statistically rigorous confidence regions in ternary diagrams and their use in sedimentary petrology. *Earth Sci. Rev.* **2002**, *57*, 211–253. [[CrossRef](#)]
59. Garzanti, E. Petrographic classification of sand and sandstone. *Earth Sci. Rev.* **2019**, *192*, 545–563. [[CrossRef](#)]
60. Folk, R.L.; Andrews, P.B.; Lewis, D.W. Detrital sedimentary rock classification and nomenclature for use in New Zealand. *N. Z. J. Geol. Geophys.* **1970**, *13*, 937–968. [[CrossRef](#)]
61. Pettijohn, F.J.; Potter, P.E.; Siever, R. *Sand and Sandstone*, 2nd ed.; Springer: New York, NY, USA, 1987; 553p.
62. Whalley, W.B.; Smith, B.J.; McAlister, J.J.; Edwards, A.J. Aeolian abrasion of quartz particles and the production of silt-size fragments: Preliminary results. In *Desert Sediments: Ancient and Modern*; Frostrick, L., Reid, I., Eds.; Geological Society: London, UK, 1987; pp. 129–138.
63. Pye, K. Shape sorting during wind transport of quartz silt grains—Discussion. *J. Sediment. Res.* **1994**, *64*, 704–705.
64. Mack, G.H. Exceptions to the relationship between plate tectonics and sandstone composition. *J. Sediment. Petrol.* **1984**, *54*, 212–220.
65. Garzanti, E.; Doglioni, C.; Vezzoli, G.; Andò, S. Orogenic belts and orogenic sediment provenance. *J. Geol.* **2007**, *115*, 315–334. [[CrossRef](#)]
66. Kumon, F.; Kiminami, K. Modal and chemical compositions of the representative sandstones from the Japanese Islands and their tectonic implications. In Proceedings of the 29th international Geological Congress Part A., Kyoto, Japan; Nishiyama, T., Fisher, G.W., Kumon, F., Yu, K.M., Watanabe, Y., Motamed, A., Eds.; VSP: Utrecht, The Netherlands, 1994; pp. 135–151.
67. Marsaglia, K.M. Basaltic island sand provenance. In *Processes Controlling the Composition of Clastic Sediments*; Johnsson, M.J., Basu, A., Eds.; Special Papers-Geological Society of America: Washington, DC, USA, 1993; pp. 41–65.
68. Le Pera, E.; Arribas, J.; Critelli, S.; Tortosa, A. The effects of source rocks and chemical weathering on the petrogenesis of siliciclastic sand from the Neto River (Calabria, Italy): Implications for provenance studies. *Sedimentology* **2001**, *48*, 357–378. [[CrossRef](#)]
69. Ingersoll, R.V.; Suczek, C.A. Petrology and provenance of Neogene sand from Nicobar and Bengal fans, DSDP sites 211 and 218. *J. Sediment. Petrol.* **1979**, *49*, 1217–1228.
70. Marsaglia, K.M. Provenance of sands and sandstones from a rifted continental arc, Gulf of California, Mexico. In *Sedimentation in Volcanic Settings*; Fisher, R.V., Smith, G.A., Eds.; SEPM Special Publication: Tulsa, OK, USA, 1991; pp. 237–248.
71. Critelli, S.; Ingersoll, R.V. Interpretation of neovolcanic versus palaeovolcanic sand grains: An example from Miocene deep-marine sandstone of the Topanga Group (Southern California). *Sedimentology* **1995**, *42*, 783–804. [[CrossRef](#)]
72. Morrone, C.; Le Pera, E.; Marsaglia, K.M.; De Rosa, R. Compositional and textural study of modern beach sands in the active volcanic area of the Campania region (southern Italy). *Sediment. Geol.* **2020**, *396*, 105567. [[CrossRef](#)]
73. Marsaglia, K.M.; Ingersoll, R.V. Compositional trends in arc-related, deep-marine sand and sandstone: A reassessment of magmatic-arc provenance. *Geol. Soc. Am. Bull.* **1992**, *104*, 1637–1649. [[CrossRef](#)]
74. Dorsey, R.J. Provenance evolution and unroofing history of a modern arc-continent collision: Evidence from petrography of Plio-Pleistocene sandstones, eastern Taiwan. *J. Sediment. Petrol.* **1988**, *58*, 208–218.
75. Zuffa, G.G. Hybrid arenites: Their composition and classification. *J. Sediment. Petrol.* **1980**, *50*, 21–29.
76. Garzanti, E.; Andò, S.; Vezzoli, G.; Dell’Era, D. From rifted margins to foreland basins: Investigating provenance and sediment dispersal across desert Arabia (Oman, U.A.E.). *J. Sediment. Res.* **2003**, *73*, 572–588. [[CrossRef](#)]
77. Critelli, S.; Le Pera, E.; Galluzzo, F.; Milli, S.; Moscatelli, M.; Perrotta, S.; Santantonio, M. Interpreting siliciclastic-carbonate detrital modes in foreland basin systems: An example from Upper Miocene arenites of the central Apennines, Italy. In *Sedimentary Provenance and Petrogenesis: Perspectives from Petrography and Geochemistry*; Arribas, J., Critelli, S., Johnsson, M.J., Eds.; Special Papers-Geological Society of America: Washington, DC, USA, 2007; pp. 107–133.
78. Cuthbert, S.J. Evolution of the Devonian Hornelen Basin, west Norway: New constraints from petrological studies of metamorphic clasts. *Geol. Soc. Lond. Spec. Publ.* **1991**, *57*, 343–360. [[CrossRef](#)]
79. Fillmore, R.P. Sedimentation and extensional basin evolution in a Miocene metamorphic core complex setting, Alvord Mountain, central Mojave Desert, California, USA. *Sedimentology* **1993**, *40*, 721–742. [[CrossRef](#)]
80. Le Pera, E.; Sorriso-Valvo, M. Weathering and morphogenesis in a mediterranean climate, Calabria, Italy. *Geomorphology* **2000**, *34*, 251–270. [[CrossRef](#)]
81. Weltje, G.J. Quantitative models of sediment generation and provenance: State of the art and future developments. *Sediment. Geol.* **2012**, *280*, 4–20. [[CrossRef](#)]
82. Garzanti, E.; Resentini, A.; Andò, S.; Vezzoli, G.; Pereira, A.; Vermeesch, P. Physical controls on sand composition and relative durability of detrital minerals during ultra-long distance littoral and aeolian transport (Namibia and southern Angola). *Sedimentology* **2015**, *62*, 971–996. [[CrossRef](#)]
83. Dutta, P.K.; Zhou, Z.; dos Santos, P.R. A theoretical study of mineralogical maturation of eolian sand. In *Processes Controlling the Composition of Clastic Sediments*; Johnsson, M.J., Basu, A., Eds.; Special Papers-Geological Society of America: Washington, DC, USA, 1993; pp. 203–209.
84. Morrone, C.; Ietto, F. Shoreline evolution and modern beach sand composition along a coastal stretch of the Tyrrhenian Sea, southern Italy. *J. Palaeogeogr.* **2021**, *10*. [[CrossRef](#)]

85. McBride, E.F.; Abel-Wahab, A.; McGilvery, T.A. Loss of sand-size feldspar and rock fragments along the South Texas Barrier Island, USA. *Sediment. Geol.* **1996**, *107*, 37–44. [[CrossRef](#)]
86. Tentori, D.; Marsaglia, K.M.; Milli, S. Sand compositional changes as a support for sequence-stratigraphic interpretation: The middle Upper Pleistocene to Holocene deposits of the Roman Basin (Rome, Italy). *J. Sediment. Res.* **2016**, *86*, 1208–1227. [[CrossRef](#)]
87. Garzanti, E.; Padoan, M.; Andò, S.; Resentini, A.; Vezzoli, G.; Lustrino, M. Weathering and relative durability of detrital minerals in equatorial climate: Sand petrology and geochemistry in the East African rift. *J. Geol.* **2013**, *121*, 547–580. [[CrossRef](#)]
88. Tortosa, A.; Palomares, M.; Arribas, J. Quartz grain types in Holocene deposits from the Spanish Central System: Some problems in provenance analysis. *Geol. Soc. Lond. Spec. Publ.* **1991**, *57*, 47–54. [[CrossRef](#)]
89. Girty, G.H. A note on the composition of plutonic sand produced in different climatic belts. *J. Sediment. Petrol.* **1991**, *61*, 428–433. [[CrossRef](#)]
90. Garzanti, E.; Andò, S.; Vezzoli, G. Grain-size dependence of sediment composition and environmental bias in provenance studies. *Earth Planet. Sci. Lett.* **2009**, *277*, 422–432. [[CrossRef](#)]
91. Morad, S. Diagenetic matrix in Proterozoic graywackes from Sweden. *J. Sediment. Petrol.* **1984**, *54*, 1157–1168.
92. McBride, E.F. Diagenetic processes that affect provenance determinations in sandstone. In *Provenance of Arenites*; Zuffa, G.G., Ed.; Springer: Dordrecht, The Netherlands, 1985; pp. 95–113.
93. Cox, R.; Lowe, D.R. Quantification of the effects of secondary matrix on the analysis of sandstone composition, and a petrographic-chemical technique for retrieving original framework grain modes of altered sandstones. *J. Sediment. Res.* **1996**, *66*, 548–558.
94. Zuffa, G.G. Optical analyses of arenites: Influence of methodology on compositional results. In *Provenance of Arenites*; Zuffa, G.G., Ed.; Springer: Dordrecht, The Netherlands, 1985; pp. 165–189.
95. Garzanti, E. Non-carbonate intrabasinal grains in arenites: Their recognition, significance, and relationship to eustatic cycles and tectonic setting. *J. Sediment. Petrol.* **1991**, *61*, 959–975.
96. Simon, S.S.T.; Gibling, M.R. Pedogenic mud aggregates preserved in a fine-grained meandering channel in the lower Permian Clear Fork Formation, north-central Texas, USA. *J. Sediment. Res.* **2017**, *87*, 230–252. [[CrossRef](#)]
97. Henares, S.; Arribas, J.; Cultrone, G.; Viseras, C. Muddy and dolomitic rip-up clasts in Triassic fluvial sandstones: Origin and impact on potential reservoir properties (Argana Basin, Morocco). *Sediment. Geol.* **2016**, *339*, 218–233. [[CrossRef](#)]
98. Pittman, E.D.; Larese, R.E. Compaction of lithic sands: Experimental results and applications. *Am. Assoc. Pet. Geol. Bull.* **1991**, *75*, 1279–1299.
99. Valloni, R.; Lazzari, D.; Calzolari, M.A. Selective alteration of arkose framework in Oligo-Miocene turbidites of the Northern Apennines foreland: Impact on sedimentary provenance analysis. *Geol. Soc. Lond. Spec. Publ.* **1991**, *57*, 125–136. [[CrossRef](#)]
100. Worden, R.H.; Mayall, M.; Evans, I.J. The effect of ductile—lithic sand grains and quartz cement on porosity and permeability in Oligocene and Lower Miocene clastics, South China Sea: Prediction of reservoir quality. *Am. Assoc. Pet. Geol. Bull.* **2000**, *84*, 345–359.
101. Harris, N.B. Diagenetic quartzarenite and destruction of secondary porosity: An example from the Middle Jurassic Brent sandstone of northwest Europe. *Geology* **1989**, *17*, 361–364. [[CrossRef](#)]
102. Milliken, K.L.; McBride, E.F.; Land, L.S. Numerical assessment of dissolution versus replacement in subsurface destruction of detrital feldspars, Oligocene Frio Formation, South Texas. *J. Sediment. Petrol.* **1989**, *59*, 740–757.
103. Morad, S.; Al-Ramadan, K.; Ketzer, J.M.; De Ros, L.F. The impact of diagenesis on the heterogeneity of sandstone reservoirs: A review of the role of depositional facies and sequence stratigraphy. *Am. Assoc. Pet. Geol. Bull.* **2010**, *94*, 1267–1309. [[CrossRef](#)]
104. Parsons, I.; Thomson, P.; Lee, M.R.; Cayzer, N. Alkali feldspar microtextures as provenance indicators in siliciclastic rocks and their role in feldspar dissolution during transport and diagenesis. *J. Sediment. Res.* **2005**, *75*, 921–942. [[CrossRef](#)]
105. Critelli, S.; Nilsen, T.H. Petrology and diagenesis of the Eocene Butano sandstone, La Honda Basin, California. *J. Geol.* **1996**, *104*, 295–315. [[CrossRef](#)]
106. De Ros, L.F.; Morad, S.; Paim, P.S.G. The role of detrital composition and climate on the diagenetic evolution of continental molasses: Evidence from the Cambro-Ordovician Guaritas Sequence, southern Brazil. *Sediment. Geol.* **1994**, *92*, 197–228. [[CrossRef](#)]
107. De Ros, L.F. Heterogeneous generation and evolution of diagenetic quartzarenites in the Silurian-Devonian Fumas Formation of the Paran Basin, southern Brazil. *Sediment. Geol.* **1998**, *116*, 99–128. [[CrossRef](#)]
108. Wilkinson, M.; Haszeldine, R.S. Aluminium loss during sandstone diagenesis. *J. Geol. Soc. Lond.* **1996**, *153*, 657–660. [[CrossRef](#)]
109. Ehrenberg, S.N. Relationship between diagenesis and reservoir quality in sandstones of the Garn Formation, Haltenbanken, Mid-Norwegian Continental Shelf. *Am. Assoc. Pet. Geol. Bull.* **1990**, *74*, 1538–1558.
110. Krainer, K.; Spötl, C. Detrital and authigenic feldspars in Permian and early Triassic sandstones, Eastern Alps (Austria). *Sediment. Geol.* **1989**, *62*, 59–77. [[CrossRef](#)]
111. Worden, R.H.; Burley, S.D. Sandstone diagenesis: The evolution of sand to stone. In *Sandstone Diagenesis: Recent and Ancient*; Burley, S.D., Worden, R.H., Eds.; Blackwell Publishing: Malden, MA, USA, 2003; pp. 3–44.
112. Morad, S. Mica alteration reactions in Jurassic reservoir sandstones from the Haltenbanken area, offshore Norway. *Clays Clay Miner.* **1990**, *38*, 584–590. [[CrossRef](#)]
113. McKinley, J.M.; Worden, R.H.; Ruffell, A.H. Smectite in sandstones: A review of the controls on occurrence and behaviour during diagenesis. In *Clay Mineral Cements in Sandstones*; Worden, R.H., Morad, S., Eds.; Blackwell Publishing: Malden, MA, USA, 2003; pp. 109–128.

114. Worden, R.H.; Morad, S. Clay minerals in sandstones: Controls on formation, distribution and evolution. In *Clay Mineral Cements in Sandstones*; Worden, R.H., Morad, S., Eds.; Blackwell Publishing: Malden, MA, USA, 2003; pp. 3–41.
115. Moraes, M.A.S.; De Ros, L.F. Infiltrated clays in fluvial Jurassic sandstones of Recôncavo Basin, northeastern Brazil. *J. Sediment. Petrol.* **1990**, *60*, 809–819.
116. Buurman, P.; Jongmans, A.G.; PiPujol, M.D. Clay illuviation and mechanical clay infiltration—Is there a difference? *Quat. Int.* **1998**, *51*, 66–69. [[CrossRef](#)]
117. Griffith, J.; Worden, R.H.; Woolridge, L.J.; Utley, J.E.P.; Duller, R.A. Detrital clay coats, clay minerals, and pyrite: A modern shallow-core analogue for ancient and deeply buried estuarine sandstones. *J. Sediment. Res.* **2018**, *88*, 1205–1237. [[CrossRef](#)]
118. Dapples, E.C. Stages of Diagenesis in the Development of Sandstones. *Geol. Soc. Am. Bull.* **1962**, *74*, 913–934. [[CrossRef](#)]
119. Dunoyer de Segonzac, G. The transformation of clay minerals during diagenesis and low-grade metamorphism: A review. *Sedimentology* **1970**, *15*, 281–346. [[CrossRef](#)]
120. Glennie, K.W. Lower Permian-Rotliegend. In *Petroleum Geology of the North Sea—Basic Concepts and Recent Advances*; Glennie, K.W., Ed.; Blackwell Scientific Publishers: London, UK, 1998; pp. 137–173.
121. McKie, T.; Williams, B. Triassic palaeogeography and fluvial dispersal across the northwest European Basins. *Geol. J.* **2009**, *44*, 711–741. [[CrossRef](#)]
122. Abbink, O.; Targarona, J.; Brinkhuis, H.; Visscher, H. Late Jurassic to earliest Cretaceous palaeoclimatic evolution of the southern North Sea. *Glob. Planet. Chan.* **2001**, *30*, 231–256. [[CrossRef](#)]
123. Vieira, M.; Jolley, D. Stratigraphic and spatial distribution of palynomorphs in deep-water turbidites: A meta-data study from the UK central North Sea Paleogene. *Mar. Pet. Geol.* **2020**, *122*, 104638. [[CrossRef](#)]
124. Humphreys, B.; Morton, A.C.; Hallsworth, C.R.; Gatliff, R.W.; Riding, J.B. An integrated approach to provenance studies: A case example from the Upper Jurassic of the Central Graben, North Sea. *Geol. Soc. Lond. Spec. Publ.* **1991**, *57*, 251–262. [[CrossRef](#)]
125. Knudsen, T.-L. Contrasting provenance of Triassic/Jurassic sediments in North Sea Rift: A single zircon (SIMS), Sm-Nd and trace element study. *Chem. Geol.* **2001**, *171*, 273–293. [[CrossRef](#)]
126. Andrews, S.D.; Morton, A.; Decou, A.; Frei, D. Reconstructing drainage pathways in the North Atlantic during the Triassic utilizing heavy minerals, mineral chemistry, and detrital zircon geochronology. *Geosphere* **2021**, *17*. [[CrossRef](#)]
127. Paul, J.; Puff, P. Das Klima des Buntsandsteins. *Schr. Dtsch. Ges. Geowiss.* **2013**, *69*, 213–221. [[CrossRef](#)]
128. Olivarius, M.; Weibel, R.; Friis, H.; Boldreel, L.O.; Keulen, N.; Thomsen, T.B. Provenance of the Lower Triassic Bunter Sandstone Formation: Implications for distribution and architecture of aeolian vs. fluvial reservoirs in the North German Basin. *Basin Res.* **2017**, *29*, 113–130. [[CrossRef](#)]
129. Weibel, R.; Geological Survey of Denmark and Greenland, Denmark. Personal communication, 2021.
130. Marín, D.; Escalona, A.; Grundvåg, S.-A.; Nøhr-Hansen, H.; Kairanov, B. Effects of adjacent fault systems on drainage patterns and evolution of uplifted rift shoulders: The Lower Cretaceous in the Loppa High, southwestern Barents Sea. *Mar. Pet. Geol.* **2018**, *94*, 212–229. [[CrossRef](#)]